NUMERICAL SIMULATION AND EXPERIMENTAL STUDY OF THE BEHAVIOUR OF VORTEX RINGS

BY

FANG HUA, M. ENG.

A thesis
Submitted to the School of Graduate Studies
in Partial Fulfilment of the Requirements
for the Degree
Doctor of Philosophy

McMaster University

NUMERICAL SIMULATION AND EXPERIMENTAL STUDY ON THE BEHAVIOUR OF VORTEX RINGS

DOCTOR OF PHILOSOPHY (1994) McMASTER UNIVERSITY

(Mechanical Engineering) Hamilton, Ontario

TITLE: Numerical Simulation and Experimental Study of the Behaviour of Vortex Rings

AUTHOR: Fang Hua, B.Sc. (Beijing Institute of Mechanical Engineering)
M.Eng.(Shanghai University of Technology)

SUPERVISOR: Dr. Brian Latto

NUMBER OF PAGES: xviii, 122

ABSTRACT

The research was directed at an understanding of the behaviour of vortex rings under more realistic and complex conditions than those considered previously. A numerical method using a control volume finite difference technique was employed to simulate vortex ring behaviour in various vessel geometries. Unlike in other studies, buoyancy effects were included. The flow behaviour of the fluids in a tank due to the formation and motion of the vortex rings was studied. Several computer models have been developed for numerical simulation of various conditions. The conditions that were simulated are: (1) the effects of injecting Reynolds number and Richardson number on the penetration of a laminar vortex ring through a stratified layer of sharp or linear temperature change along the interface; (2) the formation and motion of a single vortex ring ejected from a tube centrally located near fluid free surface of a cylindrical tank, for stratified non-Newtonian power law model fluids with Richardson numbers of 0.0, 0.01 and 0.1 and power law indices of 0.17, 0.571 and 1.5; (3) the formation and motion of primary and secondary vortex rings ejected from an orifice plate, centrally located in the bottom or middle level of a tank having thermally stratified water depth to tank diameter ratios of 1, 1.695 and 2.77, with and without a peripheral gap around the generating plate.

The numerical results showed that: (1) the penetration and trajectory of a laminar vortex ring is virtually independent of the injection Reynolds number, but primarily dependent on Richardson number; (2) laminar vortex rings in a power law fluids behave inviscidly, virtually the same as in Newtonian fluids for a certain range of injecting Reynolds numbers; (3) secondary vortex rings generated at a plate type orifice have similar trajectories and vorticity intensities to those of primary vortex rings for a trapezoidal injecting velocity-time profile. This results in the doubling of the mass transportation and most probably more efficient mixing; (4) the vorticity created at the plate periphery and also along the vessel wall can have a notable effect on the behaviour of the primary and secondary vortex rings, and so does the vorticity at region remote from the generating device. The intensity of the vorticity created in this manner is dependent on parameters such as, peripheral gaps between the impeller and the vessel wall , the orifice size, and the velocity-time profile for the generating plate. This phenomenon has not been described before and appears to be of considerable interest for both fundamental and mixing studies.

Some empirical experiments have been preformed and there appears to be good agreement with the numerical simulation studies. The flow visualization clearly displays the formation and motion of the primary and secondary vortex rings, and rolling up, transportation, transition and turbulent decay of a laminar vortex ring within its travelling

distance. Experimental results demonstrate that the behaviour of vortex rings and the interaction of primary and secondary vortex rings are very dependent on displacement-time motion profile of the generating device.

ACKNOWLEDGEMENTS

I would like to express sincere appreciation to my supervisor Dr. B. Latto for his guidance and continuous encouragement throughout the course of this study.

The appreciation is extended to Mr. Ron Lodewyks, Mr. Joe Verhaeghe and Mr. Dave Schick for their assistance in setting up the experimental apparatus.

The financial support from National Science & Engineering Research Council via graduate scholarships and a teaching assistantship from the Department of Mechanical Engineering is gratefully acknowledged.

TABLE OF CONTENTS

LIST OF FIGURES

NOMENCLATURE

C_p constant-pressure specific heat

D vortex ring diameter

D_0 orifice or tube inner diameter

F frequency of injection

g gravitational acceleration

k thermal conductivity

L_0 injecting stroke

m parameter in power law viscosity model

n power law index

P dimensionless pressure $P = \frac{p - p_0}{\rho v_*^2}$

Pr Prandtl number

R dimensionless radial coordinate $R = {}^{r}/_{r_i}$

Re injecting Reynolds number $Re = {}^{-v_* r_i}/_{\nu}$

Ri Richardson number $Ri = \frac{g \beta (T_1 - T_2) r_i}{v_*^2}$

r radial coordinate

r_i inlet tube radius

r_o tank radius

t_{in} injection time (period of injection is $0 \leq t \leq t_{in}$)

T_1 initial fluid temperature in tank upper half

T_2 initial fluid temperature in tank lower half

u radial velocity

U dimensionless radial velocity $U = {}^{u}/_{-v_*}$

v axial velocity

V_{in} dimensionless injection velocity $V_{in} = v_{in}/-v_*$

v_{in} injection velocity

v_T vortex ring translation velocity

v_* average injection velocity $v_* = \frac{1}{t_{in}} \int_0^{t_{in}} v_{in}\, dt$

V dimensionless vertical velocity $V = {}^{v}/_{-v_*}$

y axial coordinate

Y dimensionless vertical coordinate $Y = {}^{y}/_{r_i}$

Greek Letters

β volume coefficient of expansion

Γ circulation

θ dimensionless temperature $\theta = \frac{T - T_2}{T_1 - T_2}$

μ dynamic viscosity

ν kinematic viscosity

ρ fluid mean density

τ dimensionless time $\tau = {}^{t\,(-v_*)}/_{r_i}$

τ_{in} dimensionless injection time $\tau_{in} = \frac{t_{in}\,(-v_*)}{r_i}$

Δ rate of deformation tensor

τ viscous stress tensor

σ_{ij} components of dimensionless stress tensor

τ_{ij} components of stress tensor

CHAPTER 1

INTRODUCTION

The research is concerned with ring vortices generated from various circular orifice configurations. A ring vortex is a toroidal ring of rotating fluid which usually has an overall oblate spheroidal shape. The internal structure of a ring vortex can be laminar or turbulent depending on the generation conditions and the time from generation. Figure 1.1 shows a typical ring vortex and its various regions.

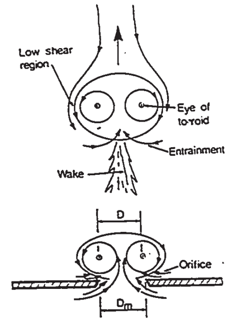

Figure 1.1 Generation of a vortex ring through an orifice.(Latto 1987)

Ring vortices can be viewed as one of the most interesting phenomena in fluid dynamics. Several properties of vortex rings are quite remarkable. Of particular interest from a practical point of view is that they are capable of transporting a parcel of fluid a considerable distance through an ambient fluid with only slight decrease in their translational velocity. This is primarily due to the fact that the fluid within the vortex ring is rotating such that at its periphery, the velocity of the fluid relative to the fluid outside the ring approaches zero. Hence, the shear rate at the periphery of a vortex ring is a very low and in essence the vortex ring basically rolls through an ambient fluid. Since the viscous shear is a function of the product of the fluid viscosity and the shear rate, and the shear rate is very low, the viscous drag is therefore very low. As a consequence of this, the viscosity has very little effect on the viscous drag for laminar vortex rings. However viscous effects can obviously affect the internal shear within the vortex ring and energy dissipation for turbulent vortex rings. Furthermore, due to the rotating boundary of a vortex ring, the form or pressure drag is relatively low.

Another remarkable feature of vortex rings is that they are directionally stable and normally travel in straight lines, although their trajectories can be affected by adjacent vortex rings and solid boundaries under certain conditions. These properties briefly indicated have led to various proposed practical applications by some authors, e.g. Turner (1960), Struchayev (1990), Baird (1979)(1992) and Latto (1987)(1989)(1992) (1993) etc. Latto, after over 13 years of experimentation with a range of liquid and liquid/slurry systems and configurations, has suggested a wide range of applications. He has also developed several types of vortex ring mixers and holds several patents on vortex ring mixers. He is at present involved in the commercialization of the mixers for the mixing of liquid and slurries, and the efficient controlled addition of solids & fluids to liquids, which is the basic requirement for many mixing processes and systems.

Much of the past work on vortex rings has been dedicated to fundamental studies of their creation and behaviour by many contributors such as Maxworthy (1977), Didden (1979), Brasseur (1986), Linden (1973), Hecht (1980) and Walker (1987) etc. The interest has primarily been related to specific aspects such as: (1) the general properties of vortex rings in their various phases of motion, e.g. formation, translation, decay, penetration through density gradients(stratification); and (2) the effects of surrounding disturbances on the path of a ring, for example the proximity of a solid boundary, and the interaction between two vortex rings. However, all previous studies on vortex rings were only limited to Newtonian fluid.

From a practical point of view in many of the proposed mixing applications of vortex rings, there is a need for a knowledge of their properties in such phases as the formation, transportation and decay, especially for non-Newtonian fluids. Another aspect which has not been given much attention, but has considerable value to a mixing process, is the generation of what may be considered as secondary vortex rings. A secondary vortex ring is primarily produced by the inertial or virtual mass effects of the fluid within or around a generating device. They can be viewed as the result of fluid which follows a plate generator, passing through the generating orifice when it is abruptly stopped, to create a vortex ring. A tube or chimney type generator, produces a primary vortex ring with a very weak secondary vortex ring which may pass back into the tube. A plate type generator however will produce both a primary & secondary ring of equal or different strength i.e. two vortex rings per stroke, or a total of four rings for a complete cycle of

a plate. Although mention has been made in the past to secondary rings, very little fundamental study has been given to requirements for the generation of these rings and their behaviour. This is particularly the case for non-Newtonian fluids.

Numerical studies of vortex rings started around 1970, which is much later than empirical and/or analytical studies due to the complexity of the problem and the lack of the required high-speed computer technology. A numerical method using the finite difference technique based on control volume is currently being employed by the author for the simulation of vortex ring behaviour for various fluids, generating devices and vessel geometries. This numerical technique appears to be a viable alternative to large scale experiments. It is felt that this approach, even though it can be expensive for asymmetrical geometries, is more economic and convenient than performing large scale empirical tests. The numerical simulation of the behaviour and application of laminar vortex rings has given unexpected results which have never been noted before and would be very difficult to demonstrate experimentally. This is the considerable value of the numerical analysis developed in this research program. Furthermore, numerical results combined with analyses may have important effects on the direction of future empirical work. It not only lets researchers design an effective and reasonable experimental scheme and arrangement, but also provides sufficient information to permit researchers to focus on to specific areas during the experimental process, in order that valuable phenomena and information would not be neglected or misunderstood.

It is quite apparent that although a great deal of effort in the past has been put into the fundamental aspects of vortex ring behaviour, there is a need for more work to be done on fundamental behaviour of vortex rings, such as formation, transportation and decay, especially in non-Newtonian fluids. Another aspect which has been given only cursory attention is the generation of secondary vortex rings, and also the penetration of vortex rings through density stratification interfaces, and their effects on mixing. This thesis attempts to address these areas.

CHAPTER 2

LITERATURE REVIEW

Vortex rings have been studied extensively by a large number of researchers over the last century. Rogers (1858) was the first one to report ring vortices formed by impulsively ejecting a puff of fluid (gas or liquid) from a circular aperture or allowing a single drop of a liquid to fall from a height of a few millimetre into a pool of the same liquid. The earlier investigations were mainly flow visualization or theoretical inviscid flow analyses. The earliest and simplest mathematical model is "Hill's Spherical Vortex" (1894) in which the moving inviscid fluid is considered to occupy a spherical envelope. Another model of ring vortices which has received considerable attention has been presented by Lamb (1933). In this case, the vorticity is assumed to be contained in a torus whose vortex ring core radius is much smaller than the mean radius of the torus about its central axis. Several previous investigators studied the formation process of vortex rings using photography such as Krutsch (1939), Okabe (1961) and Maxworthy (1977) etc. More recent research on vortex rings has expanded to a wide range of aspects. Some papers discussed experimental work closely related to the present research such as: the formation and motion of a vortex ring (Didden (1979), Brasseur (1986), Glezer (1988)); the impact of a vortex ring on a wall (Walker (1987), vortex rings traversing a fluid with a step change in density (Linden (1973), Hecht (1987)); the

interaction of several vortex rings with one another (Oshima (1978)); and fluid mixing using vortex rings (Baird, 1979, 1992) and (Latto, 1987, 1989, 1993).

2.1. THE FORMATION AND MOTION OF A VORTEX RING AND EFFECTS OF CONDITIONS

A vortex ring can be generated by ejecting a specified volume of fluid out of a tube or an orifice. As the fluid flows out of an orifice, the boundary layer separates from the sharp edge of the orifice and immediately rolls up into a spiral that gradually moves away from the edge. This spiral, which is a zone of concentrated vorticity, is the basis for the future core of the vortex ring. Meanwhile, the injected fluid outside of boundary edge spreads rapidly outward and forms the shape of a mushroom. The outer edge of the mushroom curls back into the jet of fluid emerging from the tube or orifice; this process is accompanied by the entrainment of some of the ambient fluid. The swirling mass of fluid moving away from the edge assumes the overall shape of an oblate spheroid which is composed of alternate layers of fluid from the tube or orifice and ambient fluid outside the orifice. The spheroid is slightly flattened

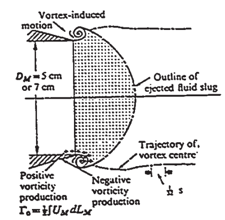

Figure 2.1 Rolling up process of a vortex ring during its generation at a tube. Maxworthy (1977).

in the direction of its motion. The rolling up process is discussed by Maxworthy (1977) and is shown in figure 2.1.

The characteristic parameters of the fully formed vortex ring are the diameter D, circulation Γ and its translation velocity v_T, as shown in many experimental investigations. The properties of the vortex ring mainly depend on (1) the generator geometry conditions: the structure of vortex ring generator and the diameter D_0 of an orifice; (2) the initial conditions: the stroke L_0 and the fluid injection velocity-history $v_{in}(t)$. The Reynolds number can be considered as a combined parameter of some of these basic parameters. The formation process of the a vortex ring is quite complicated, and there is no satisfactory theory which relates the vortex parameters for vortex ring to the generation conditions. A great deal of effort has been given to this problem, and some typical publications are reviewed here.

Maxworthy (1977) suggested that during the vortex ring formation, the ring diameter D is the function of the initial parameter L_0/D_0 over a wide range of Re ($v_* D_0/\nu$). One possible power law dependence relates the data D/D_0 to L_0/D_0. His measurements also showed that total circulation is proportional to L_0/D_0. From the flow visualization of rolling up process in figure 2.2, Maxworthy found that as the vortex ring moves away from the nozzle the flow it induces creates a secondary vortex of vorticity of opposite sign that propagates back into the nozzle and is destroyed as shown in figure 2.2(a). A similar observation was obtained for a thin orifice plate; but now as the secondary vortex moves away from the orifice the positive vorticity production ceases

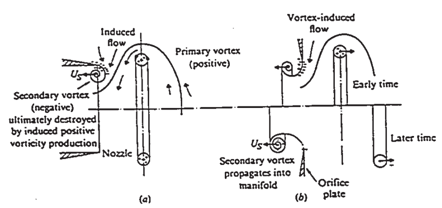

Figure 2.2 Rolling up process for tube-generator (a) and orifice-generator (b). Maxworthy (1977)

and the ring is not destroyed, as shown in figure 2.2(b).

In order to obtain more detailed information on the flow near the nozzle for a realistic production of vortex circulation, Didden (1979) using laser Doppler anemometry measured the unsteady velocity field in the nozzle-exit plane during the rolling up process. His data show that both the diameter of the formed vortex ring and circulation near nozzle wall depend on the parameter L_0/D_0 and are independent of the average injecting velocity v_* within a certain Reynolds number range. Didden's work revealed two valuable conclusions. Firstly, the starting flow around the nozzle exit produces a larger velocity $v > v_*$ near the nozzle wall, causing a larger vorticity flux into the vortex ring, specially at small time t (see figure 2.3). This is the reason why the circulation calculated in the simple slug model, in which a constant injection velocity $v_{in} = v_*$ over the nozzle cross section is assumed during the piston stroke, is much smaller than the

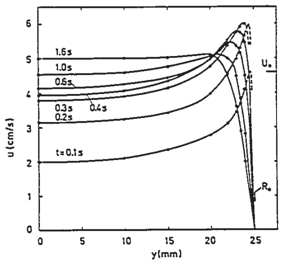

Figure 2.3 Axial velocity u verses radial distance y in the tube-exit plane x=0, U_o=4.6cms-1, R_o=25mm: inner tube wall. Didden (1979)

circulation measured under the virtual situation. Secondly, the net vorticity flux into the vortex ring is considerably diminished by the negative vorticity of the external boundary layer, which is produced by the flow of the rolling up vortex at the outer nozzle wall (see figure 2.4).

It is obvious that L_o/D_0 is a important parameter in the formation of the vortex ring. Baird et al (1979) recommended that for a most efficient laminar vortex ring the L_o/D_0 ratio should preferably be the range 0.7 to 2.8. Later Latto (1987) suggested that this range should be $1.5<L_o/D_0<3.5$ with an optimum value of L_o/D_0 of about 2.8. Virtually any value for L_o/D_0 will result in the generation of a ring vortex, but outside the

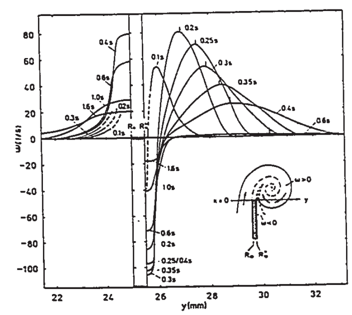

Figure 2.4 Vorticity ω verses radial distance y at x=0, U_o=4.6cms^{-1}. Didden (1979)

suggested range a vortex ring will be very weak for small values of L_o/D_0, and when L_o/D_0 is larger than 3.5 an initial primary vortex ring develops and leaves the orifice when it has reached an optimum size and then another vortex ring is formed immediately behind the primary vortex ring. The following ring overtakes the primary ring and is ingested by it which normally results in an instability of the primary vortex ring with either its destruction or a deflection from its original path.

As mentioned previously, the characteristics of a vortex ring depend strongly on the geometry boundary condition. Since all of the vorticity essential to the existence of a vortex is generated in the boundary layer prior to the formation of the ring, different geometries will produce different amounts of vorticity. Furthermore, in the case of a tube type generator (in figure 2.5), vorticity of opposite sense is generated on the outside of the tube orifice by the boundary layer formed from the entrained flow, passing over the solid surface, thereby impeding the influx of entrained flow and diminishing the net available vorticity. These effects will result in the generation of vortices with different sizes and different propagation speeds,

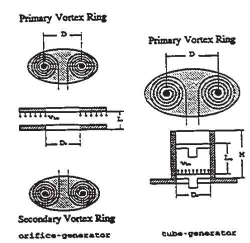

Figure 2.5 Two types of vortex ring generator

as well as differences in internal flow fields.

Two very common structures of vortex ring generation and boundary conditions are showed in figure 2.5. The data of Irdmusa and Garris (1987) show that tube-generated vortex rings tend to have a slower translation velocity and larger volume than orifice-generated vortices for a given injection condition and orifice diameter. They suggested that the exit boundary condition can have a very large effect on the entrainment and the partition of kinetic energies of translation and rotatic. . Irdmusa and Garris pointed out that vortex rings with minimal amounts of kinetic energy of rotation can be generated by proper attention to boundary conditions and by using pulses of very short duration.

Another strong effect on the formation and developing of a vortex ring is the injection velocity v_{in} history. The result of Didden's (1977) work resulted in figure 2.6 which shows that different injecting velocity programs will lead to different characteristics of vortex rings, even when using an identical average injection velocity v_-. In practical mixing experiment using vo:tex rings, Latto (1987) found the sinusoidal motion of plate with an orifice can not produce an

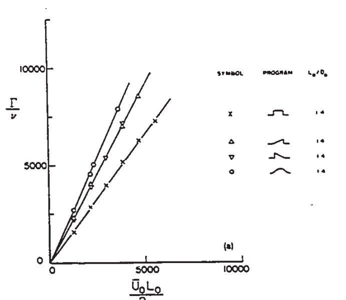

Figure 2.6 Circulation for the laminar vortex rings produced with various injection velocity programs.

energetic vortex ring. He suggested that the motion of plate should be a gradual rise followed by a dwell period and a very fast drop with further dwell period, by the use of a particular generating cam profile.

A large part of the literature on vortex rings deals with laminar vortex rings. However, some literature deals with turbulent vortex rings. It is natural that questions are asked regarding turbulent vortex rings, such as, what conditions are required for the generation of turbulent vortex rings or the transition from an initial laminar vortex ring to a turbulent vortex ring, and what are the characteristics for turbulent vortex rings? The following papers investigate these problems and give some answers.

The transition from a laminar vortex ring to turbulent ring may precede or follow an azimuthal instability of the vortex core. This instability involves the appearance and amplification of azimuthal waves around the circumferen.e of the core. As the vortex moves away from the generator, the waves may subsequently break down to turbulence if their amplitude is large enough. Maxworthy (1977) observed that both the onset and break down to turbulent azimuthal core instability occurred close to the orifice of the vortex generator when the Reynolds number (based on v_- and D_0) of an initially laminar vortex ring was increased.

Brasseur (1986) obtained information on the evolution characteristics of vortex rings over a wide range of Reynolds numbers using flow visualization experiments. He used an orifice diameter D_0 to tank diameter ratios in the range 0.16 - 0.64, which would appear to be too large to eliminate the effect of tank wall on the vortex rings. Brasseur found that vortex rings can be divided into three groups depending on the Reynolds number, characterized by the rate at which circulation is lost continuously from the vortex ring to its wake. At Re $\geq$ 20000, rapid turbulent diffusion of vorticity from the core and convection into the wake produces a 1/t decrease in translation velocity. The total circulation is found to decrease in a manner similar to that of the velocity. At Re $<$ 1000 to 2000, the much slower process of molecular diffusion results in a $1/t^{\alpha}$ decrease in the translation velocity, and a decrease in circulation within the vortex ring, where α = 0.13 to 0.27. In between, there is a very wide range of intermediate Reynolds numbers, however the vortex ring behaves 'inviscidly', with almost no decrease in translation velocity or circulation.

Glezer's work (1988) categorizes and combines all the generating conditions for vortex rings, and then sets up a relationship between these conditions and characteristics of vortex rings in a very clear and simple way. His experimental data were used in a survey which verified that the two dimensionless parameters Γ_0/ν and L_0/D_0 are often sufficient to characterize the behaviour of a particular vortex ring during its formation. The results of this survey are represented in a transition map shown in figure 2.7. The crosses represent vortex rings that remained laminar during at least part of the available range of observation in the tank. The filled circles represent vortex rings that became turbulent essentially as soon as they were formed. The shaded band denotes separation of initial laminar and initial turbulent vortex rings. This transition map identifies the conditions leading to the generation of vortex rings that are initially either a laminar ring,

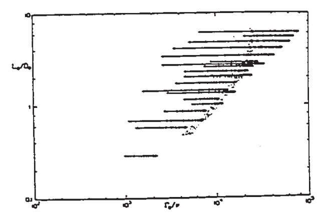

Figure 2.7 Dimensionless transition map. Glezer (1988)

which may or may not undergo instability and transition to turbulence, or a turbulent ring. Data from other investigations (Turner (1957), Grigg and Stewart (1963), Johnson (1970), Didden (1977), Glezer (1981)) using vortex generators of different geometries, are consistent with that transition boundary of map. It is also suggested that amplification and breakdown of an inherent azimuthal instability of the vortex core are greatly accelerated, thus leading to an early transition to turbulence, when the wavelength of the vortex sheet instability is less than L_0. Since the instability wavelength of the spiralling vortex sheet increases when v_* is decreased (L_0 is inversely proportional to v_* for a fixed Γ_0/ν), by keeping Γ_0/ν fixed and giving an orifice diameter D_0, it is possible to produce a ring that remains laminar throughout the available range of observation, when the instability wavelength is larger than L_0.

Comparing laminar and turbulent vortex rings produced from an orifice generator, Widmayer (1972) found that at corresponding downstream positions, the translational velocity of turbulent vortex rings is substantially less than that of laminar vortex rings, and ring diameter growth of the turbulent vortex rings is several times that of the laminar vortex rings. This is because more mass is entrained into turbulent vortex rings. Unlike

laminar vortex rings which have only a very slight loss of circulation, turbulent vortex rings have a relatively large loss of circulation. Based on these different properties between laminar and turbulent vortex rings, Widmayer strongly suggested that in any application of vortex rings where mass transport, impulse transport, or energy transport is required, turbulent vortex rings should be avoided. He suggested that efficient use of vortex rings in such application can only be realized if the rings employed are laminar. However, for fluid mixing a turbulent ring really produces mixing in its wake it progresses through a fluid and provided rings reach the required location, a turbulent vortex ring may be more desirable than a laminar one. The liquid-liquid dispersion is one of examples. (Latto et al. (1994))

There are other factors affecting the characteristics of the vortex ring. One such factor is an interface due to stratified fluid with two different densities or a density gradient. Linden (1973) was apparently the first to investigate this kind of situation for a vortex ring penetrating down into a stratified layer having a sharp change in density gradient. He studied vortex rings that could hardly penetrate the stratified interface. When the ring impacts the interface, the surface is deflected downwards by the ring, and the ring is flattened, while retaining circular symmetry about a vertical axis through the centre of the ring. After the interface reaches its points of maximum deflection, the buoyancy forces cause the interface to recoil, and the ring to collapse and denser fluid to be ejected into the upper layer to mix with the fluid in the ring. Linden found that at the maximum penetration depth of the ring at the interface, the diameter of the region of contact between the ring and interface and the rate of turbulent entrainment are

functions of the Froude number based on the density difference across the interface. However, the penetration in this case means the penetration of a vortex ring at the interface, and not complete passage of a ring through the interface.

Dahm (1989) et al. experimentally and numerically studied the dynamics of the interaction between a vortex ring with lengthscale 'a' and circulation Γ encountering a interface of thickness δ across which the fluid density increases from ρ_1 to ρ_2. Their results indicated that this interaction is governed by two dimensionless parameters, namely $(a/\delta)A$ and R, where $A=(\rho_2-\rho_1)/(\rho_2+\rho_1)$ and $R=(a^3g/\Gamma^2)$. For thin interface ($\delta \leq a$), the interaction is governed only by the parameters A and R. In the paper, Dahm et al. presented excellent detailed photographs of the interaction between vortex rings and an interface and a vortex ring's penetration with backflow, for small values of AR. Their experimental results were in agreement with their numerical calculations. However their concern and focus were only on the internal and external changes of a vortex ring and the deformation of the interface under the interaction with various parameters. The penetration depth of a vortex ring presented in their paper is not the maximum penetration through a interface until itself destructs.

Both Honji (1976) and Maxworthy (1977) investigated vortex ring penetration in a stratified layer with a gradual change in density profile. A vortex ring projected vertically upward into the fluid with density varied with the depth was observed by Honji. It was seen that as a vortex ring reaches an interface it is considerably elongated in the vertical direction due to gravitative effect. Maxworthy considered a stratified fluid with a linear density profile in almost the whole depth of test fluid. The vortex rings in Maxworthy experiment travelled downwards, however similar observation to Honji's on the decrease of ring diameter was obtained, with a slowing of a ring's velocity until its eventual destruction. Maxworthy explained the reasons of these phenomena. The decrease in diameter is a consequence of pieces of the core being torn away and mixing into the outer flow and wake since buoyancy force destabilizes core/outer flow interface. The buoyancy force torque and opposite vorticity production due to the different density among the core, outer ambient fluids reduce the total ring circulation, and decelerates a ring.

Hecht et al. (1980) studied turbulent vortices in fluids with linear and discontinuous density stratifications. They found that stratification has a profound effect on the radius of a vortex ring descending into a stably stratified fluid, and the descent velocity of a vortex ring is near constant or decreases monotonically with increasing penetration into a stably stratified fluid, depending upon the type of stratification present (discontinuous or linear).

A considerable amount of the research has been done by Latto and Baird on the application of vortex rings. The research was mainly concerned with the destratificaton of different density fluids or liquid/slurry system. Their work and results are described in Section 2.3. on the application of vortex rings for mixing.

2.2. NUMERICAL STUDIES OF VORTEX RINGS

Since about 1970, papers have appeared describing numerical studies on the behaviour of vortex rings traversing a fluid. One of the earliest papers was by Whitehead (1968) whose numerical procedure resulted in a detailed streamline and vorticity-line description of the initial development stage of viscous vortex rings.

Busnaina and Lilley (1983) conducted a numerical study on the use of an axial flow propeller for mixing a thermally stratified fluid. The propeller was located above the interface between the warm and cold fluid, which is called the thermocline. The flow of high quality epilimnion water, was directed downwards and was mixed locally by the propeller which achieved local destratification and improved release water quality in the vicinity of low level release structures. The author of this thesis believes that vortex rings will provide a more energy efficient means of mixing stratified fluids, since the fluid along the entire path of the vortex rings is mixed, and vortex rings are able to penetrate far into the thermally stratified fluid.

Hecht et. al. (1980) examined the behaviour of turbulent rings traversing a stratified fluid, although they did not consider the vortex ring formation process. They developed an axisymmetric wake computer code to simulate the penetration of a ring into the stratified layer. With their program, they were able to predict the slow down and decrease in the size of the ring. Their prediction agreed very well with the experimental data for a ring that was travelling in a stratified layer with a linear change in density

gradient, However, their prediction for the case with sharp change in density gradient was not as accurate as that for a linear density change.

Friebel and Rath (1987) simulated the behaviour of laminar vortex rings from the formation phase to the viscous decay by solving the two dimensional Navier-Stokes equations in cylindrical coordinates, neglecting buoyancy effects. The influence of various parameters on the vortex generation process was investigated. The behaviour of vortex rings in the vicinity of different obstacles, walls and free surfaces was simulated. In addition, the interaction of two vortex rings travelling along the same axis is studied by them. Their numerical simulations are in good agreement with their own measurements and experimental data in the available literature.

The formation and transport of vortex rings in a thermally stratified fluid were studied numerically by Papple et al. (1991) and Latto et al. (1990) using a control-volume based finite difference method. The formation of vortex rings was simulated by single (1991) or periodical (1990) injection of a quantity of the fluid through a tube centrally located near a free surface in a tank initially containing a stably stratified fluid with a sharp temperature change along the interface. Buoyancy effects were considered in their work. The mixing behaviour in the tank, due to the formation and motion of the vortex rings, was studied. Their results showed that the ability of a buoyant vortex ring to penetrate into a tank with a step change in density is a function of the Richardson number Ri, which is the ratio of buoyancy force and inertia force. For low values of Ri the buoyant vortex rings can penetrate the high density fluid causing significant mixing.

However, for $Ri > 0.1$, the vortex ring cannot penetrate the high density fluid and mixing can only occur at the interface. The result obtained in their work may be useful in the design and analysis of vortex ring mixers.

2.3. MIXING APPLICATION OF VORTEX RINGS

The extensive fundamental studies of vortex rings have been accompanied by several practical applications. Johnson et al. (1982) designed special jet nozzles for drilling coal and rock with water jets. The ring vortices are used to increase cavitation in order to get better drilling rate. On the laboratory scale, a "vortical chimney" was investigated by Turner (1960) and Baker (1970) for using vortex rings to release pollutant or industrial wastes intermittently into a heights of several hundred meters.

In 1972, a feature article in the non-technical literature written by Kendig suggested some other possible applications, such as destroying thermocline (boundary layers in water where the temperature changes sharply), thus promoting circulation and oxygenation; intercepting and dissipating the so-called tip vortices left by larger planes, thus making the skies around our major airports considerably safer spaces in which to fly; and aerating deep water and sewage etc.

Recently, Struchayev (1990) further investigated to use vortex rings in transporting 'passive' impurities over large distances without large losses of such impurities from the zone of their localization in the rings. A technique is applied in their experiments for rapid evaluation of the efficiency of dispersed impurity mass transport.

Mixing of liquids is one of most common operation in the industries involved with the manufacture and processing of liquids and solid suspension. It eliminates discontinuities or gradients of physical properties in a mass of liquid by the circulation and transfer of material from one location to another. A number of factors determine the efficiency of a particular method of mixing, such as mixing time, ability to produce a homogeneous or dispersed liquid, and the power consumption. Numerous methods for mixing and agitation of fluids have been used from standard rotation and oscillation impellers to complex agitator configurations. However, these traditional mixing methods quite often have a low efficiency and other disadvantages. Baird et al. (1979) investigated mixing of stratified fluids by vortex rings both in test tank of his laboratory and in field tests at the Hamilton (Ontario) Harbour. The laboratory tests revealed the energy efficiency of mixing to be a function of vortex ring path length and Froude number, which is expressed as density difference of stratified fluids. Those tests indicated that in terms of energy utilisation, vortex rings can be considerably more efficient than impellers in mixing stratified liquids.

Although there have been a lot of publications on the theory and experiments of vortex ring generation, growth and propagation, and obviously these studies are useful in the analysis of the behaviours of individual vortex ring, they are not completely useful for analyzing or designing bulk mixing system which use the continuous generation of vortex rings. Latto has devoted a great deal of effort to the study of vortex ring mixing

and mixers for a quite long time and made considerable progress in this area of interest.

After research on various aspects of vortex rings for over ten years, Latto (1987) considered one of more important parameters to be L_0/D_0 which is the ratio of the effective plug length of fluid being ejected to the diameter of the orifice. The recommended value is between 1.5 to 3.5 for the efficient productions of vortex rings, and the optimal value is about 2.8. His studies show that a oscillating plate vortex ring mixer can be used very well for mixing many liquids & slurries, giving excellent homogeneous dispersion of the fluid with very low energy input in comparison with traditional rotating and oscillating impellers.

Latto (1987, 1989-1993) has developed three novel forms of vortex ring mixers, which he has patented. These are a suspended plate mixer, a self contained oscillating plate mixer, and a tube (chimney) type mixer. These units have been and are being tested at industrial sites in Canada and the U.S.A.. A very large number of both quantitative and qualitative experiments, as well as a numerical study using a finite difference analysis of the flow equation, have been done over a ten year period. His studies indicate quite clearly that vortex ring mixers are a novel approach to the mixing of fluids, being very effective and efficient for industrial mixing. Furthermore, these types of vortex ring mixers have a very wide range of applications, such as the mixing of stratified liquids and slurries, the efficient addition of liquids or solid additives, the mixing of very high temperature liquids e.g. molten metals, the separation of solid suspensions, aeration of liquids, destratification of liquids/slurries and liquid-liquid extraction (Baird et al.(1992),

Rama Rao et al.(1994) and Latto et al.(1994)). The simplicity of their design and adaptability makes them very convenient to use and maintain.

When studying the effects of buoyancy on the behaviour of vortex rings in destratification of liquids, the Richardson number Ri is an important parameter that must be considered. Ri is the function of two parameters, the density difference between stratified liquids or slurries and vortex ring translation velocity or average injection velocity of vortex rings. The mixing or agitation effectiveness when buoyancy is a factor, is very dependent on the Ri number for the particular system.

More recently Latto(1990) conducted a series of larger scale experiments using a tube type vortex ring mixer for de-stratification of cold/hot water system in a 1110L capacity rectangular and 2000L capacity cylindrical mixing tanks. The data obtained from these experiments further show the effectiveness and energy efficiency of vortex ring mixers, and show that it is apparent that the penetration of a vortex ring for mixing or stratification of a liquid system are primarily dependent on the Richardson number and virtually independent of the injection Reynolds number.

CHAPTER 3

PENETRATION OF VORTEX RINGS IN STRATIFIED FLUIDS

3.1 INTRODUCTION

As previously stated, over the last century an appreciable amount of work and publications have been directed towards various aspects of vortex rings. The emphasis has primarily been related to theoretical analyses and basic experiments on the formation and behaviour of vortex rings especially laminar rings. Very few publications have addressed the use of vortex rings for practical applications. In 1972 Mattingly suggested a number of applications for vortex rings (Kendig, 1972) but these do not appear to have been extensively tried until Baird (1979) investigated the use of vortex rings for destratification of lakes; a little later, Latto developed vortex ring mixers for a wide range of applications, such as the mixing of sedimentary slurries, Newtonian and non-Newtonian liquids and the gasification of liquids.

The real problem associated with the use of vortex rings is an understanding of the operating characteristics of the vortex ring generating devices. These characteristics require a knowledge of various parameters related to vortex ring generation and propagation, such as the injection time-velocity characteristics for the efficient generation of a vortex ring, the role of viscosity and geometric parameters, the frequency at which vortex rings can be generated without interaction between successive vortex rings, the distance a ring will travel if unhindered, and the depth of penetration of vortex rings into miscible and immiscible stratified fluid layers. This latter aspect of the penetration of vortex rings into stratified layers is very important when mixing sedimented liquid slurries and in the destratification of large bodies of liquids.

3.2 EXPERIMENTAL APPARATUS

In order to compare the numerical results with empirical data an apparatus was designed and constructed. A photograph of the experiment apparatus is shown in figure 3.1. This apparatus is composed of a 0.3 by 0.3 m^2 cross section by 2 m deep plexiglass tank with a capacity of 185 L, which is supported on a steel frame as shown in figure 3.2. A tube type vortex ring generator located on the top of the tank projects vortex rings from just below the free surface of the water towards the bottom of the tank. The

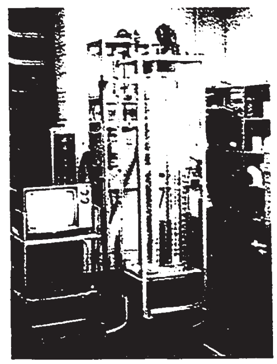

Figure 3.1 Photograph of experimental apparatus with a tube generator.

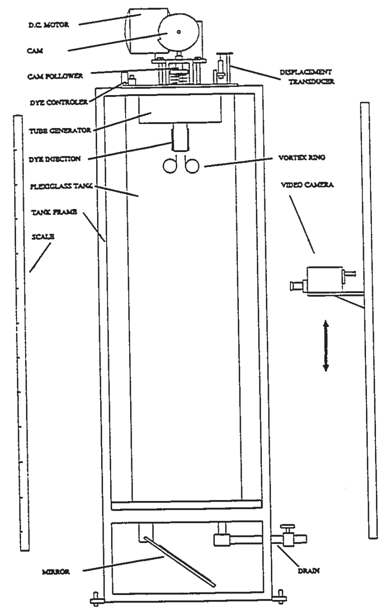

Figure 3.2 Schematic of the apparatus with tube generator.

velocity-time profile of vortex ring generation is controlled by a cam mechanism having a particular profile, which is driven by a variable speed D.C. motor. A displacement transducer attached to the generating diaphragm is used to record the motion of the generating diaphragm and thus measure a vortex ring generation fluid displacement profile. Diluted food dye is injected into the shear layer just outside the wall at the mouth of the generating tube via two capillary tubes. This permits flow visualization of the vortex ring. A mirror system is located below the floor of the tank, which permits the axial observation of a vortex ring as it progresses towards the floor of the tank.

A video camera is used to record the process of generation and the path of a vortex ring in the tank until it reaches the bottom of the tank, or disintegrates. The camera is located on a platform which can be raised or lowered using a pulley system driven by a variable speed D.C. motor, to follow and record the displacement of the vortex ring with respect to the orifice. After an experiment is recorded using the video recorded, a digital video frame grabber, HRT 512-8, is used to analysis these images and obtain information about the location and core diameter of the vortex ring and their trajectories after they are generated.

3.3 NUMERICAL METHOD

A cylindrical tank configuration was used for the numerical simulation. A diagram of a cylindrical tank which contained an initially stationary fluid is shown in figure 3.3(a). The fluid was stably stratified, having a higher density fluid in the lower half

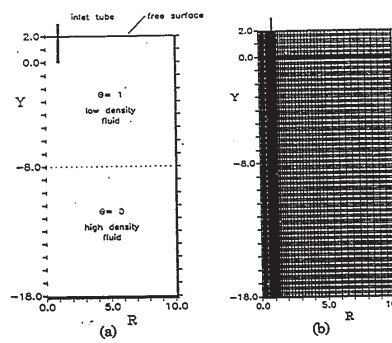

Figure 3.3 Fluid initial state of the tank (a) and control volume mesh (b).

than in the upper half. The formation of a vortex ring was simulated numerically by rapidly injecting a quantity of the lower density fluid through a small diameter inlet tube centrally located near the surface. This injected fluid was taken to have a Prandtl number Pr=7.0, corresponding to that for water at ambient temperature of about 20^{0}C. The inlet tube had a radius of one unit, and was inserted 2 units into the fluid. The cylindrical tank radius was 10 units, and the liquid was 20 units deep.

The velocity within the inlet tube was assumed radially uniform at the height of the fluid surface (Y=2). This uniform velocity was then varied as a function of time, as indicated in figure 3.4. A reference velocity v_* was defined by time averaging this injection velocity over the period of injection $0 \leq t \leq t_{in}$. Note for time $\tau \geq \tau_{in}$ the injection velocity equals zero.

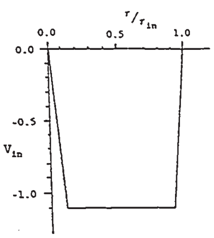

Figure 3.4 injection velocity vs. time.

During this injection phase, the vorticity near the exit of the inlet tube is high. When the fluid injection is stopped, a vortex ring forms which then travels away from the inlet tube toward the tank bottom. A photograph of a typical fully formed laminar vortex ring is shown in figure 3.5. The location of maximum vorticity is defined as the eye of the vortex ring. The vortex ring tail(wake) is also shown on this diagram. As the vortex ring moves, some fluid originally contained in the ring is left behind in the tail(wake).

Figure 3.5 A full developed laminar vortex ring.

To simulate numerically the formation and behaviour of these vortex rings, a control-volume based finite-difference technique (Patankar's SIMPLER technique) was employed to solve the continuity, Navier-Stokes and energy equations in cylindrical coordinates. This technique

employed a control-volume approach to discretize the governing equations. The velocity control-volumes were staggered with respect to the control-volumes for the pressure and temperature. The fluid was incompressible, with constant properties. The solution was assumed to be axisymmetric, and laminar. The Boussinesq approximation, i.e. the fluid density ρ is treated as a constant in all terms in the equations of motion except the one in the external force, is employed for the buoyancy term in vertical direction momentum equation. These dimensionless governing equations are as follows:

$$\frac{1}{R}\frac{\partial}{\partial R}(RU)+\frac{\partial V}{\partial Y}=0$$

$$\frac{\partial U}{\partial \tau}+U\frac{\partial U}{\partial R}+V\frac{\partial U}{\partial Y}=-\frac{\partial P}{\partial R}-\frac{1}{Re}\left[\frac{1}{R}\frac{\partial}{\partial R}\left(R\frac{\partial U}{\partial R}\right)-\frac{U}{R^2}+\frac{\partial^2 U}{\partial Y^2}\right] \tag{1}$$

$$\frac{\partial V}{\partial \tau}+U\frac{\partial V}{\partial R}+V\frac{\partial V}{\partial Y}=-\frac{\partial P}{\partial Y}-\frac{1}{Re}\left[\frac{1}{R}\frac{\partial}{\partial R}\left(R\frac{\partial V}{\partial R}\right)+\frac{\partial^2 V}{\partial Y^2}\right]+Ri\theta$$

$$\frac{\partial \theta}{\partial \tau}+U\frac{\partial \theta}{\partial R}+V\frac{\partial \theta}{\partial Y}=\frac{1}{PrRe}\left[\frac{1}{R}\frac{\partial}{\partial R}\left(R\frac{\partial \theta}{\partial R}\right)+\frac{\partial^2 \theta}{\partial Y^2}\right]$$

The strength of the generated vortex ring is intimately related to the velocity profiles at the end of the inlet tube during the injection stage. For this reason it was necessary to use a very fine mesh near the inner surface of the inlet tube to accurately calculate these profiles. For accurate results, it was necessary to use a fine mesh in the path of the vortex rings, and particularly near the generating tube inlet. The results in this thesis were obtained using a medium mesh or a coarse mesh. The medium mesh has 65 control volumes in the radial direction, and 167 in the vertical direction. Selected results were also obtained using coarse meshes with half the medium resolution, that is

33 control volumes in the radial direction and 85 in the vertical direction, to evaluate the numerical accuracy.

One parameter which is of primary importance is the dimensionless injection time τ_{in}. There is a single injection phase lasting over the time interval $0 \leq \tau \leq \tau_{in}$. This parameter is a measure of the volume of fluid injected through the inlet tube into the tank. The dimensionless volume of fluid injected into the tank during the injection phase is given by $\pi\tau_{in}$. This was obtained by integrating over the injection time the inlet tube area multiplied by the injection velocity.

Based on experiments by Baird, Wairegi and Loo (1977), Rohatgi, Baird and Wairegi (1979) and by Latto (1987), the optimal value of the injection time for tube type generators is approximately 5.5. For smaller τ_{in} ($\tau_{in}<4$) the resulting rings are weak, while for larger τ_{in}($\tau_{in}>7$) the flow resembles a jet rather than a vortex ring.

3.4 EXPERIMENTAL AND NUMERICAL RESULTS

The numerical results shown in figure 3.6 are very remarkable in that there are distinct velocity peaks in the vicinity of the tube wall at outlet. There is agreement, for injection velocity profile at outlet of the tube during injection, between the computational results of this work and the experimental data of Didden (shown in figure 1.4), who used a laser doppler anemometer for the velocity measurements. Figure 3.6 shows the decrease of injection velocity at the tube outlet at different times after it reaches the peak

value during injection. It can be seen that a high velocity gradient in the wall boundary layer for a tube generator produces a strong vortex ring and assists in its separation from the generating tube. The great moment of vorticity is concentrated on a very small area which is called the vortex ring "eye" next to the tube wall at outlet.

A very typical numerical result is given in figure 3.6 which shows that different injection velocities at the inlet of the tube will lead to notable difference in the injection velocity distribution at the outlet of the tube. Consequentially the formation and transportation properties of a vortex ring are definitely dependent on the injecting velocity profile at the inlet of the generating tube. This sensitivity of vortex ring behaviour to the motion or velocity of the injection will be discussed in detail in Chapter 4. Both the peak velocity near wall and average injection velocity at outlet from the tube during injection for a trapezoid velocity profile at inlet as shown in figure 3.6(a) are larger than those for a triangular velocity profile as shown in figure 3.6(b). Figure 3.7 shows a comparison of the vortex ring vorticity intensity and distance it has travelled from the orifice between type (a) and type (b). The higher velocity peak i.e. larger velocity gradient near the generating tube wall produces larger vorticity intensity, while a larger average injecting velocity at outlet of the tube makes a vortex ring travel longer distance from the outlet during the certain time, shown in figure 3.7(a).

A typical numerical simulation results showing the effects of injection frequency on the behaviour of a vortex ring is shown in figures 3.9 through 3.11. Under the condition of the same fluid volume ejected into the tank and the same input energy with a constant injection time, three different ejection frequency models F=1, F=2 and F=4 (see figure 3.8) are employed in the numerical simulation. The corresponding ejection velocity vs. time profiles are shown in figure 3.8. Figures 3.9, 3.10 and 3.11 present a series of vorticity contours created by vortex rings being ejected from the tube generator for injection frequencies of F=1, F=2 and F=4 respectively. From the data for the distance travelled by a vortex ring for a given time, it is apparent that the results for F=2 and F=4 are better than for F=1, and that the case when F=2 gives the best result. Comparing the cases when F=1, F=2 and F=4, it is clear from the data in figure 3.9-3.11 that a vortex ring will travel faster for the condition when F=2 than the other cases, since it hits the tank bottom after a period of ten times the injection time, but when F=1 or F=4 they do not do so. This fact shows there must be a optimal value for the injection frequency to achieve optimal use of vortex rings for various industrial applications, such as fluid mixing and mass transport.

Figure 3.12 gives a graph of radius of the "eye" and position of the vortex ring with respect to the injection time, created using a computer model. It can be seen from figure 3.12(a) and 3.12(b) that the depth of penetration into the lower fluid is virtually unaltered when the injection Reynolds number is increased tenfold, whilst keeping the Richardson number constant. Furthermore, when comparing the graphs in figure 3.13(a) and 3.13(b) it is obvious that increasing the Richardson number while keeping Re constant, has a considerable effect on the penetration distance. As Ri is increased the depth of penetration decreases until a value of Ri is reached when essentially no penetration occurs. In this numerical simulation, two different density gradient along the

interface were investigated, a sharp interface and a gradual density gradient, were used as shown in figure 3.13. The temperature distributions cross the interface of thermally stratified water are shown in figure 3.13(b). From the computational results there is no difference between them for the penetration depth and trajectories of vortex rings.

The Richardson number is obviously a very important parameter, whereas the injection Reynolds number is not so, when considering the mixing and de-stratification of liquid layers and sedimented slurries. It should be appreciated that the Reynolds number as defined, is based on injection conditions, which are a convenient criteria, and not the local Reynolds number based on the velocity and diameter of the travelling vortex ring, or a Reynolds number based on the distance from its generation point. However it can be expected that the behaviour of a laminar vortex ring would be relatively independent of the injection Reynolds numbers as defined.

Figure 3.14 shows the comparison of vortex ring penetration data (Strange (1991)) for the hot/cold water and the brine/water systems. It can be seen that there is good agreement between the data, and the numerical results are in agreement with the empirical data. Since there is a peripheral gap between tube type generator and tank wall, the actually average injecting velocity from the tube orifice is only 35%-70% of the theoretically average injecting velocity which was used to calculate the Ri shown on figure 3.14, this makes the penetration of a laminar vortex ring in figure 3.14 is smaller than that in figure 3.21 without gap between tube type generator and tank wall.

When a vortex ring passes through the interface of a stratified fluid, its size has not big change for a range of Ri<0.1 and the radius of that vortex ring has just a little bit difference from the original one (see figure 3.15), it is also found from numerical simulation that the vortex ring moves significantly faster in this region than in the other density regions, as clearly shown in figure 3.16. The data of Rama Rao et al. (1994) on a vortex ring penetrating the interface of a immiscible water/kerosene stratified two phase fluid is in agreement with this work. The velocity of the vortex ring vs time can be easily obtained from the trajectory data of a vortex ring computed in the numerical simulation for a stratified cold/hot water system. Figure 3.15 shows the vortex ring displacement vs time dimensionless and a table of the data. It is clear that the slope of the displacement-time curve close to the interface when Y=8 is larger than that at any other location. In correspondence with this, the velocity of the vortex ring through the interface reaches the largest dimensionless value 2.65 compared with about 0.5-0.6 in any other location, as shown in figure 3.16. Furthermore this largest value for the velocity is also much larger than the average dimensionless injection velocity of 1.1. This result is similar to the experimental measurements of Baird et al. (1992).

Several experiments were performed using the new experimental apparatus shown in figure 3.2 having a tube type generator. Flow visualization was used to observe the formation and transportation of laminar vortex rings, their transition until their turbulent decay or destruction on the bottom of the tank, as shown in the typical series of pictures in figure 3.17(A-R). Before the injection of fluid some dye is ejected from the two capillary tubes as shown in figure 3.17(A), in order to observe the vortex ring formation.

Figure 3.17(B) shows the process when fluid is ejected out of the tube orifice and flow separation at the boundary layer causes rolling up the vortex ring core at the sharp edge of the tube outlet. As the injection is accelerated, the rolled spiral vortex ring core moves away from the outlet. After its generation and during its forward motion the vortex ring entrains ambient fluid to enlarge its volume, however some fluid in the vortex ring is also discharged into its wake. Thus its volume increases, but not at the rate of entrainment, and its contents are diluted. A typical full developed laminar vortex ring is stabiy travelling downwards as shown in figure 3.17(E). Initially, the dyed vortex ring core was in a plane parallel to the direction of motion through the centroid of the vortex ring, which can be observed that in figure 3.18(G). The dye at the vortex ring core has a rotating motion along a circle which is called vortex core ring, in a counterclockwise direction when viewed from above. The motion quickly results in a vortex ring with a completely dyed annular core, as shown in figure 3.18(H-K). Obviously the vortex core ring is always present for these conditions, but is invisible without the dye. The dyed vortex core ring with circular motion shown in figure 3.18(K,L) is very stable and there is no wave motion to its circular motion for this particular case. As was mentioned in some papers, the transition from a laminar ring to a turbulent ring may precede or follow an azimuthal instability of the vortex core. This instability involves the appearance and amplification of azimuthal waves around the circumference of the core as the vortex ring moves. Figures 3.18(K-L) and 3.19(M) show a vortex ring which is continuously moved down for a period of time with a circular vortex core ring. When the vortex ring is close to the bottom of the tank the diameter of the circular vortex core ring gradually increases until the vortex ring hits the bottom, as shown in figures 3.19(N-O) and 3.20(P). Finally, when a vortex ring hits the bottom it rebounds and then turbulently disperses whilst rapidly increasing its radius until it eventually decays with an appreciably large diameter at impact.

Experimental data for the penetration of a laminar vortex ring generated at a tube orifice and moving downwards through a cold/hot water stratified fluid system is presented in figure 3.21. It is shown that these penetration data are in good agreement with those of Ho (1991), Strange (1991) and Rama Rao et al (1994). Ho and Strange's data were obtained in experiments in which a laminar vortex ring was ejected from a tube orifice upwards through a cold/hot water or water/brine system. The data of Rama Rao et al. were for the penetration of laminar water vortex rings ejected from a tube-type generator downwards through a water/isopar stratified two phase fluid system.

3.5 ANALYSIS AND DISCUSSION

The empirical data for the penetration depth of a vortex ring into a stratified layer shown in figure 3.21 are in good agreement with pervious experimental data. It also verifies Ho's following correlation in the form X_p/R vs. Ri. Ho used a regression analysis to correlate his and Strange's data for penetration of vortex rings through a steep density gradient. Ho obtained the following equation:

$$\frac{X_p}{R}=-29.7\log_{10}Ri-22.7$$

where $0.17>Ri>0.027$.

This relationship can be used to predict the maximum penetration depth of a vortex ring travelling in a stratified layer with a sharp density gradient. It shows that a vortex ring will not be able to penetrate an interface i.e. $X_p/R = 0$, when Ri=0.17. On the other hand, it also shows that when $Ri \rightarrow 0$, $X_p \rightarrow \infty$, however it is virtually impossible to obtain an infinite penetration. This corresponds to the results of a vortex ring travelling in an ideal fluid with uniform density and no viscosity.

Both experimental measurements and numerical results show that the penetration and trajectory of a laminar vortex ring are independent of the injection Reynolds number when Richardson number is constant, but are highly dependent on the Richardson number. A large Ri, if $Ri > 0.1$, represents a larger buoyancy force i.e. drag force on a vortex ring, which resists the vortex ring penetrating the interface and forces it back to the fluid from whence it was generated. A small Ri means that the inertial force is considerably larger than the buoyancy force and the vortex ring has enough kinetic energy to penetrate the interface. The smaller the Ri, the larger the distance of penetration of a vortex ring through an interface. Basically Ri is a function of the average velocity of injection (strictly, it should be the translation velocity of vortex ring just prior to the interface) for a given stratified fluid and a given vortex ring generation device. Therefore, for a fluid system has a high $\Delta\rho$, in order to make $Ri \rightarrow 0$ to achieve a deeper penetration of a vortex ring, either the generation velocity must be high or the generating orifice diameter must be relatively small.

Basically, it is quite easy to generate vortex rings, but it is considerably more

complex to generate vortex rings effectively for a particular application, such as fluid mixing and mass transportation. This is because many factors will affect the behaviour of a vortex ring. One factor is the injection velocity profile discussed in Section 3.4. Another factor is the injection frequency. In principle, for practical mixing within the practical operating range of a generating device, a series of vortex rings can be ejected from the orifice and they will not hit each other up to a certain generating frequency. It was clearly observed from the experiments that a vortex ring can follow another ring in a vortex ring street without particular effect each other with a frequency of generation of up to 10 Hertz. Latto (1992) has suggested that a form of the Strouhal number is a particular parameter for predicting the conditions for a street of vortex rings, that is $v/fD_m > 1.0$ where v is the velocity of the vortex ring, which is less than $0.5v_*$, f is the frequency of generation and D_m is the minor diameter of the vortex ring. However, It is worthwhile noting that it seems that the faster the generation frequency up to a practical operating limit of say 10 Hz, the better the mixing or mass transportation, but may not be strictly correct. In fact, there is a appropriate generating frequency (or frequency range) for a given vortex ring generation and its circumstance to make vortex rings themselves more efficient for a particular industry application. The result shown in figures 3.9 to 3.11 is a typical example verifying this contention.

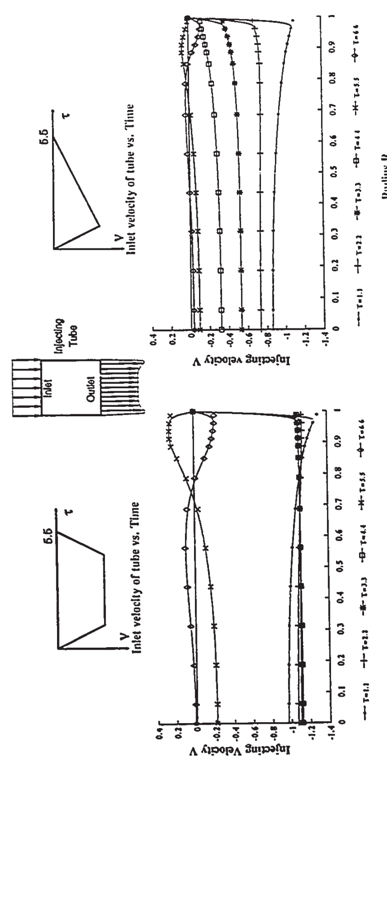

Figure 3.6 Velocity profiles in outlet of tube vs. time for two types of velocity profiles in inlet (dimensionless)

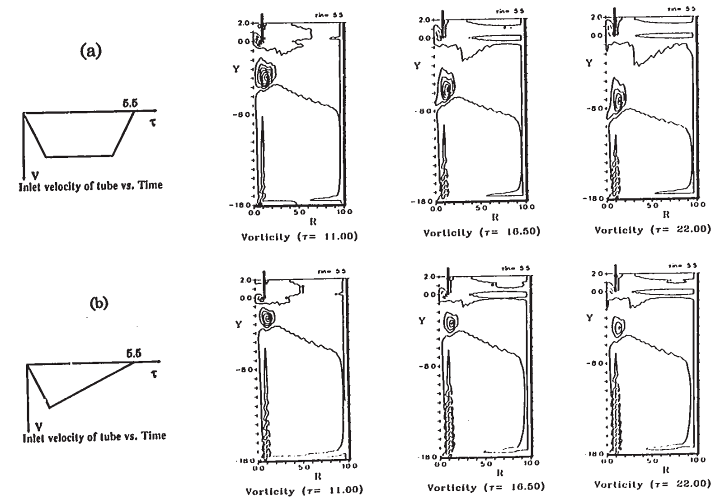

Figure 3.7 A series of vorticity contour plots for a tube generator with two types of injecting velocity profiles at the inlet of the tube.

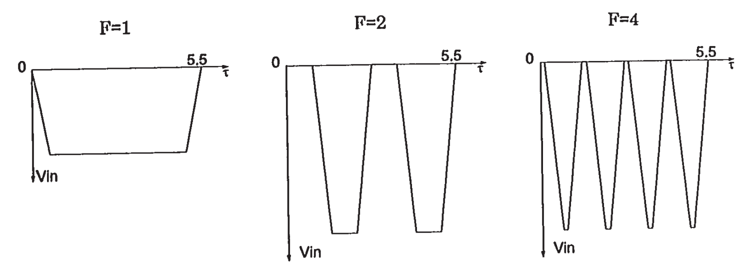

Figure 3.8 Three types of injecting velocity profiles, designated F=1, F=2 and F=4 for a tube generator.

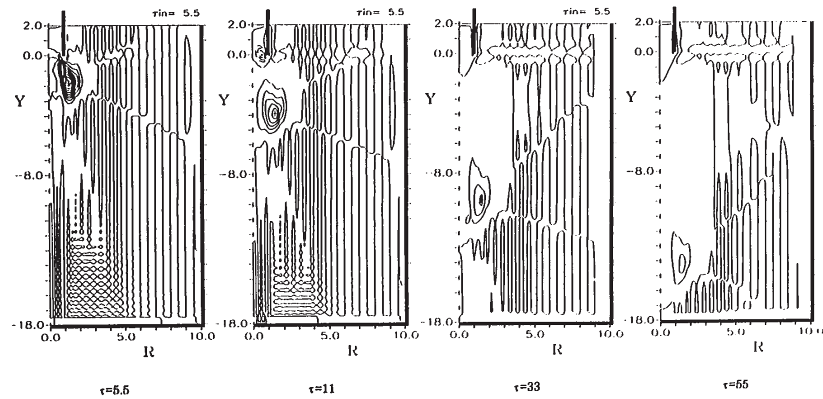

Figure 3.9 A series of vorticity contour plots for case F=1 injecting velocity profile, Re=10000 and Ri=0.0.

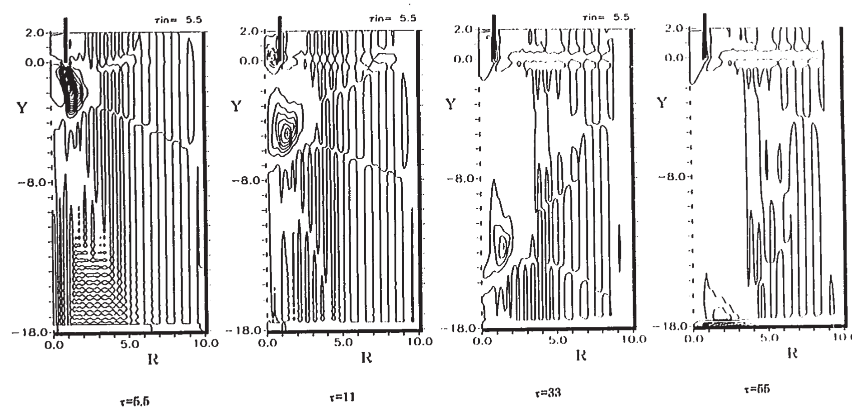

Figure 3.10 A series of vorticity contour plots for case F=2 injecting velocity profile, Re=10000 and Ri=0.0.

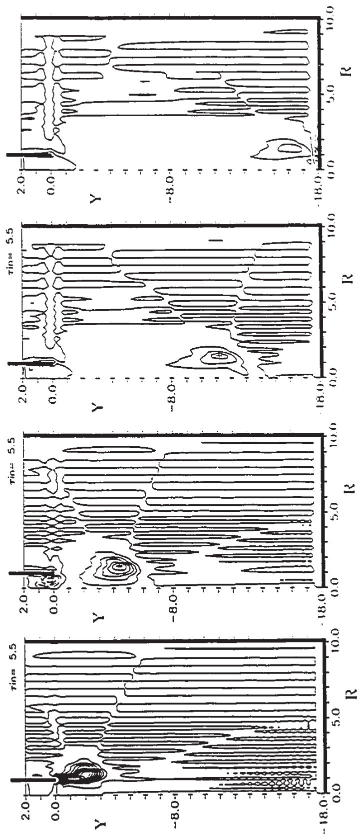

Figure 3.11 A series of vorticity contour plots for case F=4 injecting velocity profile, Re=10000 and Ri=0.0.

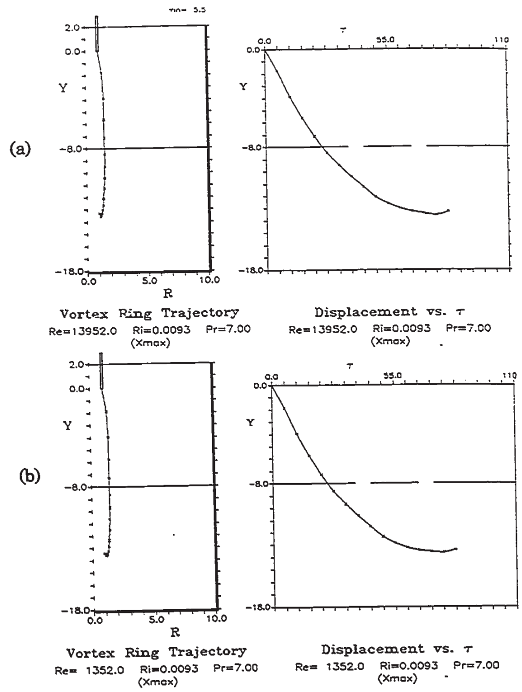

Figure 3.12 Plots showing the same trajectory & displacement of a vortex ring with time for a ten fold difference in Reynolds number.

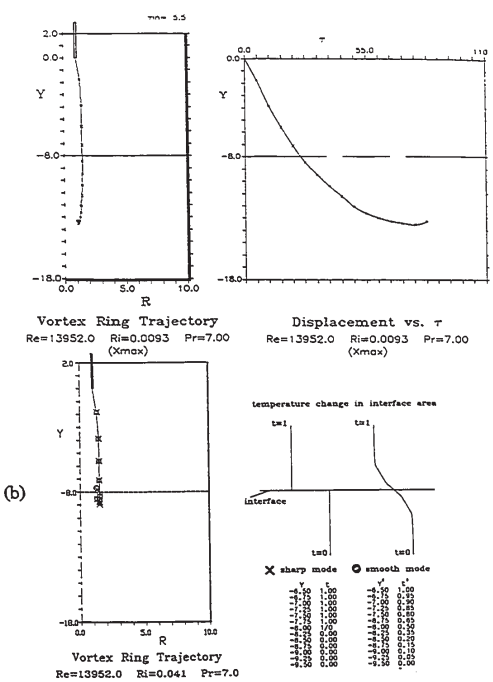

Figure 3.13 Plots showing a notable difference in the trajectory of a vortex ring when the Richardson number is changed from 0.0093 to 0.041.

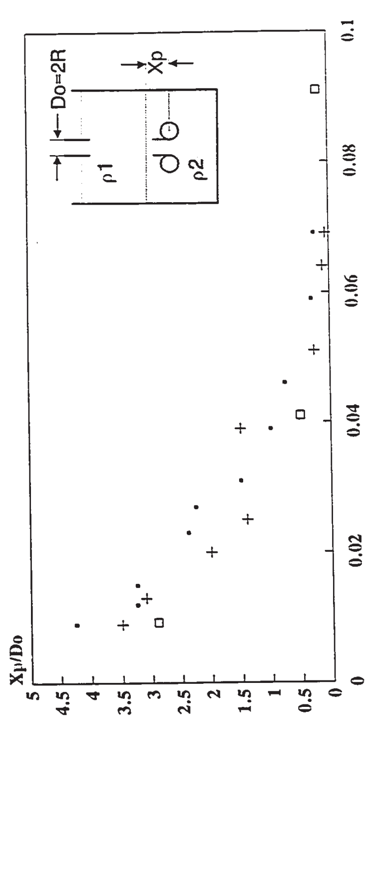

Figure 3.14 Empirical and numerical data for vortex ring penetration through a sharp density stratification.

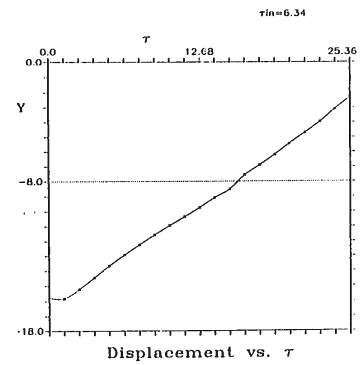

NUMERICAL DATA FOR VORTEX RING THROUGHT
A STRATIFIED FLUID INTERFACE
(dimensionless parameter)

No.	Time	Radius ratio of ring eye & orifice	Vortex ring hight	Ring velocity	Ringeye vorticity
1	0.0	1.0	-16.70	0.0	-68.00
2	1.268	1.0	-16.81	-0.038	-34.20
3	2.536	1.08	-16.21	0.473	-4.78
4	3.804	1.11	-14.44	0.607	-3.23
5	5.072	1.24	-13.68	0.623	-2.77
6	6.340	1.28	-12.92	0.578	-2.62
7	7.608	1.27	-12.22	0.562	-2.26
8	8.876	1.28	-11.65	0.528	-2.07
9	10.144	1.27	-10.92	0.497	-1.89
10	11.412	1.28	-10.33	0.486	-1.74
11	12.680	1.28	-9.72	0.481	-1.69
12	13.948	1.28	-9.08	0.506	-1.49
13	15.216	1.28	-8.50	0.467	-1.42
14	15.374	1.27	-8.41	0.566	-1.41
15	15.533	1.27	-8.33	0.505	-1.40
16	15.691	1.27	-8.27	0.379	-1.39
17	15.850	1.27	-7.85	2.660	-1.43
18	16.008	1.27	-7.82	0.189	-1.46
19	16.167	1.28	-7.74	0.605	-1.46
20	16.325	1.28	-7.63	0.694	-1.48
21	16.484	1.28	-7.60	0.462	-1.48
22	17.752	1.30	-6.83	0.628	-1.55
23	19.020	1.30	-6.10	0.660	-1.54
24	20.288	1.30	-5.44	0.654	-1.54
25	21.556	1.31	-4.69	0.691	-1.53
26	22.824	1.32	-3.85	0.664	-1.50
27	24.092	1.30	-3.09	0.678	-1.49
28	25.360	1.31	-2.28	0.631	-1.52

Figure 3.15 Vortex ring eye displacement (Y) vs time (τ) (dimensionless) for a cold/hot water system with Re=17711, Ri=-0.122.

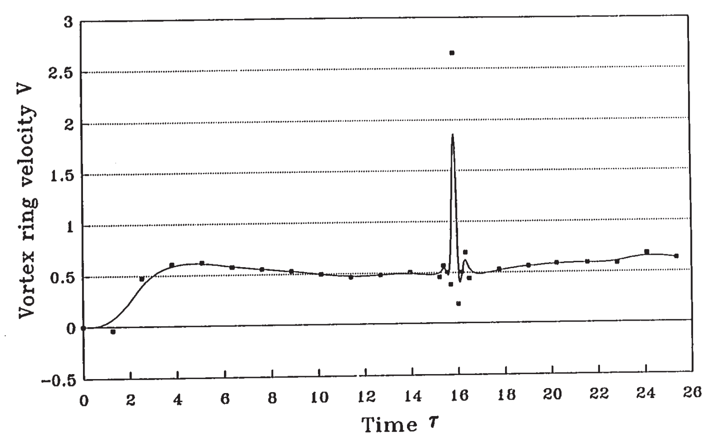

Figure 3.16 Velocity of a vortex ring eye vs time (τ) (dimensionless) for Re=17711, Ri=-0.122.

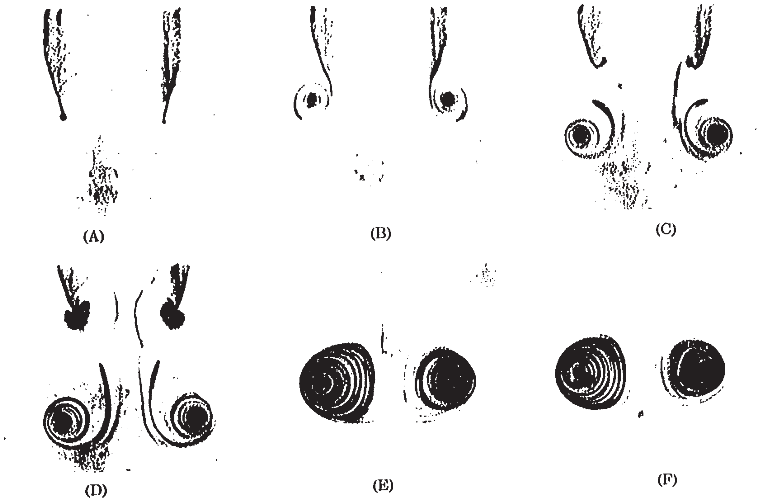

Figure 3.17 A series of pictures (A-F) of a vortex ring from its formation, transportation in decay in water of a tank with a tube type generator.

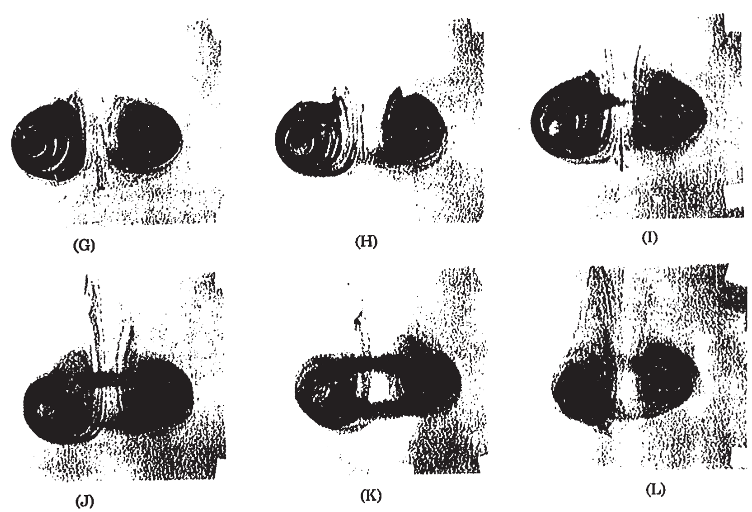

Figure 3.18 A series of pictures (G-L) of a vortex ring from its formation, transportation to decay in water of a tank with a tube type generator.

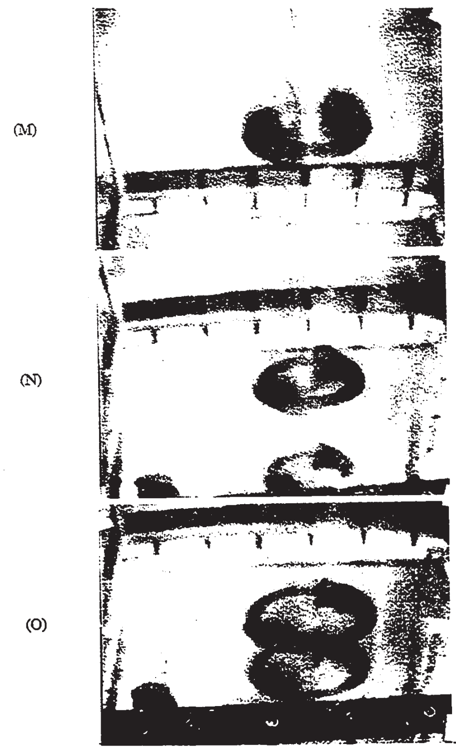

Figure 3.19 A series of pictures (M-O) of a vortex ring from its formation, transportation to decay in water of a tank with a tube type generator (see figure 3.2).

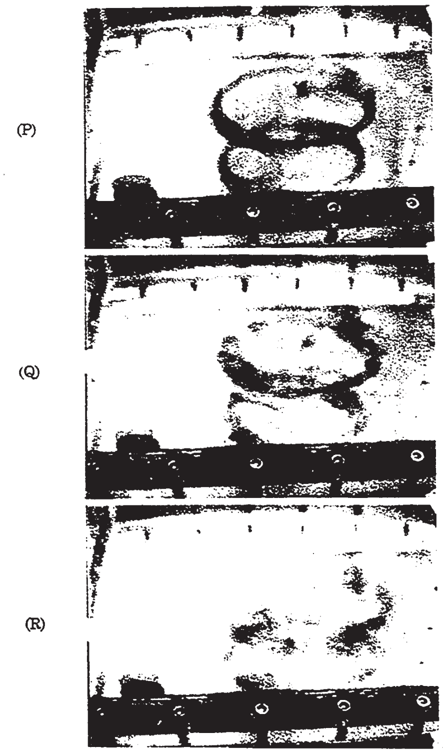

Figure 3.20 A series of pictures (P-R) of a vortex ring from its formation, transportation to decay in water of a tank with a tube type generator (see figure 3.2).

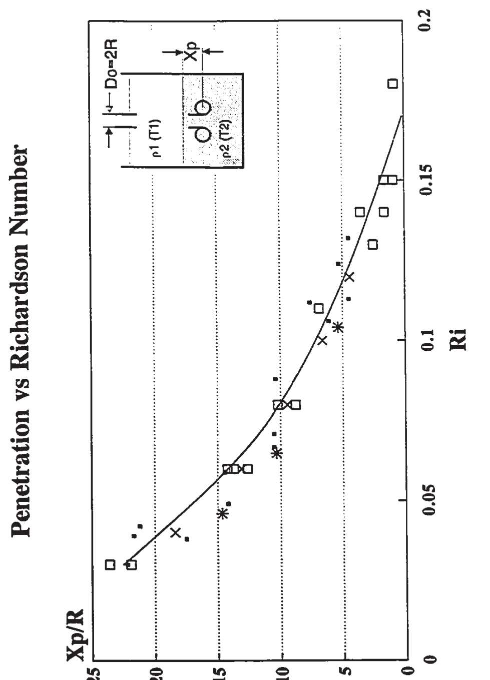

Figure 3.21 Empirical data for vortex ring penetration through a density stratification.

CHAPTER 4

SECONDARY VORTEX RINGS GENERATED AT ORIFICES

4.1 INTRODUCTION

For over a century, data have been published on various aspects of vortex rings. But as previously stated very little has been directed towards particular aspects of vortex rings. When a mechanical device such as an orifice plate is impulsively moved to generate vortex rings, as shown in figure 4.1, a second or secondary vortex ring may be generated, basically due to inertial effects of the fluid following the device. In a plate type generator, the secondary vortex ring can be quite strong and clearly visible. A complete oscillation cycle of a plate type orifice vortex ring generator can produce two primary and two secondary vortex rings. This is

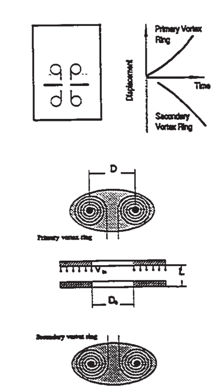

Figure 4.1 Primary & secondary vortex rings generated from an orifice plate.

usually not so for a tube generator in which fluid is impulsively discharged from the tube mouth. Only one primary vortex ring is emitted from the tube and a relatively weak secondary ring travels into the generator tube, per cycle of liquid oscillation.

When using a plate type vortex ring mixer the secondary vortex rings are quite important for mixing/agitation process. As stated before, an oscillating plate type vortex ring generator can produce four rings per cycle of the plate and therefore generate vortex rings at a rate four times the oscillation frequency of the generator. The mass transport is therefore significantly higher (up to four times) than that for a tube type generator. However, it must be realized that a tube type generator produces a larger vortex ring than that from an orifice plate generator, which partially offsets the disadvantage that only one vortex ring is produced per cycle for a tube type generator. Furthermore, not all the fluid displaced by a plate type generator is used to create a vortex ring. The peripheral flow created by the fluid which has not passed through the orifice may enhance localized mixing, but it may also create peripheral or wall vortices. These vortices may or may not be valuable to mixing, as discussed later.

In order to efficiently design vortex ring mixers an accurate assessment of the vortex ring behaviour for various types of generator and the prediction of mass transfer is very important. This is also true for the interaction of vortex rings with localized vorticity and turbulence in the fluid media, both adjacent and distant from the generating device.

4.2 EXPERIMENTAL APPARATUS

A photograph and a schematic diagram of the experimental apparatus are shown in figures 4.2 and figure 4.3 respectively. The system is comprised of a 0.31 m square cross section tank having a maximum depth of 1.52m. The tank has two opposite plexiglass sides for flow visualization and the other two sides are aluminum.

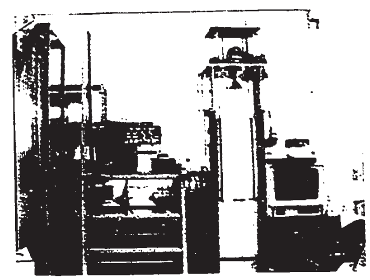

Figure 4.2 Photograph of experimental set up with an orifice generator.

A 30.5 cm square orifice plate onto which various sizes of aluminum orifice plates or a plexiglass tube type orifice can be attached, is used to generate vortex rings. The plate is driven by four rods which are attached to the corners of the plate, from the top of the tank (see in figure 4.4). The aluminum lip of the orifices and a metal ring on the lip of the tube type generators is used to generate hydrogen bubbles using electrolysis; small tubes at the periphery of the orifice are used for injecting dye for flow visualization. Both the hydrogen bubbles and the dye are essentially injected into the fluid shear layer at the edge of the orifice. Outside the tank on the front plexiglass face, a scale is set vertically,

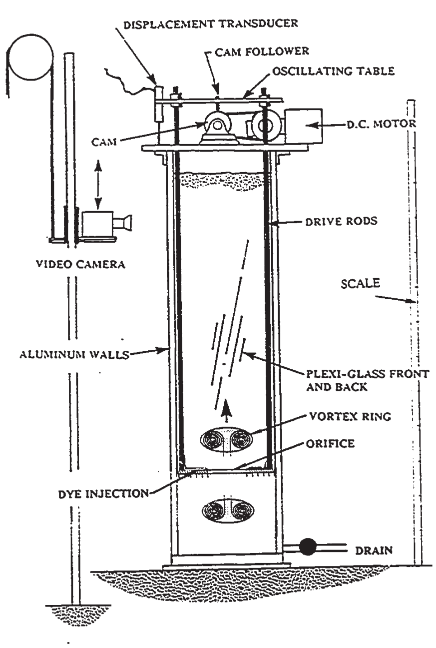

Figure 4.3 Schematic of experimental set up with an orifice generator.

which can be used as a visual measure of the location of a vortex ring. A video camera is used to record the process of generation and the path and behaviour of a vortex ring from generation to disintegration. The video camera is mounted on a support platform which can be driven vertically parallel to the axis of the tank, at predetermined speeds to follow a vortex ring using a variable speed D.C. motor in conjunction with an electric clutch.

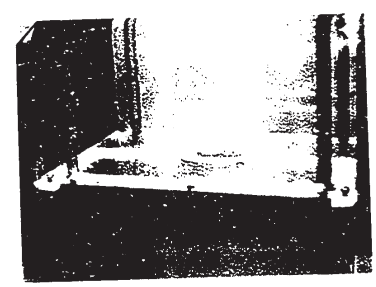

Figure 4.4 Photograph of an orifice-generator plate.

A variable speed D.C. motor located at the top of the tank drives a cam having a particular profile which drives the upper platform, which in turn drives the four rods connected to the orifice plate. The plate is thus driven up and down to generate vortex rings at the orifice. The displacement and velocity of the plate is measured using a Hewlet-Packard displacement transducer (model 7DCDT-500), which is connected to an oscilloscope and also a data acquisition system "notebook" for further computer processing. After an experiment is recorded using the video recorder, a digital video frame grabber, HRT 512-8 is used to analyse these images and obtain information about the location and core diameter of a vortex ring and its trajectories after it is generated.

4.3 NUMERICAL METHOD

In order to simulate the formation and behaviour of a vortex ring ejected from an orifice generator, a computer model using a finite-difference technique was developed and employed to solve the continuity, Navier-Stokes and energy equations in cylindrical coordinates. This technique employed a control-volume approach to discretize the governing equations. The velocity control-volumes were staggered with respect to the control-volumes for the pressure and temperature. The fluid is considered to be incompressible, with constant properties. The problem was assumed to be axisymmetric, and laminar. The Boussinesq approximation, by which the fluid density ρ is assumed constant, was employed in all terms with the exception of the buoyancy term in vertical direction momentum equation. In dimensionless form, these governing equations, which are the same as equations (1) but different boundary conditions, are as follows:

$$\frac{1}{R}\frac{\partial}{\partial R}(RU)+\frac{\partial V}{\partial Y}=0$$

$$\frac{\partial U}{\partial \tau}+U\frac{\partial U}{\partial R}+V\frac{\partial U}{\partial Y}=-\frac{\partial P}{\partial R}-\frac{1}{Re}[\frac{1}{R}\frac{\partial}{\partial R}(R\frac{\partial U}{\partial R})-\frac{U}{R^2}+\frac{\partial^2 U}{\partial Y^2}] \tag{3}$$

$$\frac{\partial V}{\partial \tau}+U\frac{\partial V}{\partial R}+V\frac{\partial V}{\partial Y}=-\frac{\partial P}{\partial Y}-\frac{1}{Re}[\frac{1}{R}\frac{\partial}{\partial R}(R\frac{\partial V}{\partial R})+\frac{\partial^2 V}{\partial Y^2}]+Ri\theta$$

$$\frac{\partial \theta}{\partial \tau}+U\frac{\partial \theta}{\partial R}+V\frac{\partial \theta}{\partial Y}=\frac{1}{PrRe}[\frac{1}{R}\frac{\partial}{\partial R}(R\frac{\partial \theta}{\partial R})+\frac{\partial^2 \theta}{\partial Y^2}]$$

Two non-uniform meshes were used in this computation work: a medium resolution mesh with 65 control volumes in the radial direction, and 167 in the vertical direction; and a coarse resolution mesh with 33 control volumes in the radial direction and 85 in the vertical direction. The initial conditions are shown in figure 4.5a, and the pressure and temperature control volume mesh in figure 4.5b.

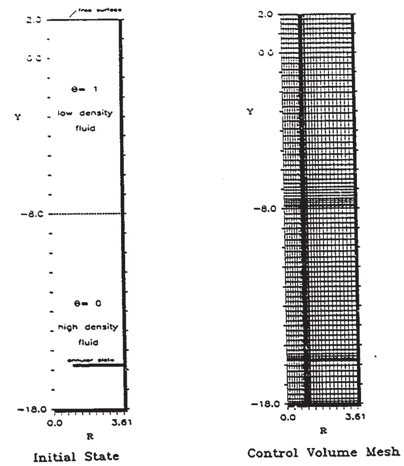

Figure 4.5 (a) Initial state of cylindrical tank; (b) Control volume grids.

The strength of each generated vortex ring is intimately related to the velocity profiles near the orifice plate during the injection stage. For this reason it was necessary

to use a very fine mesh near the plate surfaces to accurately calculate these profiles. For accurate results, it was also necessary to use a fine mesh in the path of the vortex rings.

4.4 EXPERIMENTAL & NUMERICAL RESULTS AND DISCUSSION

Four typical vortex rings generated during a complete cycle of an orifice plate type vortex ring generator centrally located in a tank can be seen in the two photographs in figure 4.6. When the orifice plate moves down, it produces a primary vortex ring which travels upwards, and a secondary vortex ring which travels downwards. When the plate returns up to its initial position, it produces a primary vortex rings which travels downwards, and a secondary vortex ring which travels upwards, thus for a complete cycle four vortex rings are produced.

Experiments have clearly shown that under a specific motion of the generating plate the primary vortex rings can pass through the secondary vortex rings, which has been observed by Oshima (1975) before. This is because the primary rings are moving at a higher velocity than the secondary rings and can overtake the secondary rings. However it is very surprising that the primary ring can pass through a secondary ring without any apparent damage to itself. This phenomena is shown in the series of photographs in figures 4.7(A-F) and 4.8(G-L).

Also as expected, the velocity and behaviour of the rings are very dependent on

the displacement-time motion profile of the generating device. Different displacement-time profiles will produce different generation velocity and acceleration profiles. An example of this is given in figure 4.9 which presents a typical profile obtained from a displacement transducer for a given run. In order to efficiently produce an energetic vortex ring the acceleration-time profile is most important. The magnitude of the acceleration of the generating plate or fluid motion in the orifice will profoundly affect the vorticity intensity and other properties of a vortex ring. Both the initial acceleration and the final deceleration of the generating plate will affect the properties of vortex rings and the velocity, size and motion of the primary and secondary vortex rings, and therefore the interaction of these two types of rings.

These aspects of vortex ring interaction and generation are very important when using vortex rings to mix/agitate fluids, and in the control of vortex ring mixers for a wide range of applications. For example, in order to produce equally intensive primary and secondary vortex rings and avoid interaction between the rings, and therefore obtain efficient mixing relatively remote from the generating device, the displacement-time profile of the generating device must have a particular form. Furthermore, the particular motion of the generating device during a complete cycle, can be designed to produce controlled mixing. For example, when using an orifice plate generator a stronger upwards motion than a downwards motion may be required for destratification of a liquid/liquid system with a larger density in the bottom or a liquid/solid system such as sedimentary slurry. Another example is the controlled depth of penetration of vortex rings when using a tube generator, which may be used to cause mixing of a fluid without agitation of underlying sediment. Thus by having a knowledge of the behaviour of vortex rings with respect to generating motion, an optimal control of the mixing process and an intelligent interactive mixer design are possible.

Typical numerical data presented in Figures 4.16 and 4.17 show the velocity vectors and vorticity contours of primary and secondary vortex rings at selected times from generation. When an orifice plate moves down, a primary vortex ring is ejected up. When the plate is abruptly stopped, the inertial force of the fluid behind the generating plate produces a secondary vortex ring which travels in an opposite direction to that of the first one. A plate type generator will produce both a primary & secondary ring with almost equal strength and approximately similar trajectory i.e. two vortex rings per stroke, or a total of four rings for a complete cycle of a plate under the condition of a typical plate injecting motion. Consequently, a plate type generator can produce four times as many as vortex rings as a tube type generator, even though the size of the vortex rings is smaller than that of those generated with a tube, the total volume contained by these vortex rings is much larger than that of a vortex ring form the tube. Therefore, a plate will create more efficient mass transfer and mixing than a tube generator. This is especially the case for the mixing of sedimentary slurries or stratified fluids, when a plate generator can be located near an interface, two vortex rings containing the particulate matter and/or dense phase material will be projected upwards and two vortex rings containing the dilute phase will be projected downwards per cycle

of the generating plate, and thus these cause rapid destratification of the materials. Furthermore, as pointed out by Latto an orifice generator has a simple geometry and structure, may be made of a flexible material, and is easy to install and maintain whilst being energy efficient.

In order to assess the actual fluid flux through the orifice compared with the peripheral loss when the generating plate is moved one way, with a small peripheral gap between the generating plate and the wall of the tank, the velocity profile across the orifice at the exit plane was measured at various time intervals using hot film anemometry by Ho (1992). The resulting velocity-time data were integrated to give volumetric flow rates with respect to time. The gap between the plate and the tank wall was nominally about 2% of the side of the plate. It was found that the quantity of fluid that passed through the orifice was considerably less than the fluid displaced by the plate, due to flow around the periphery of the plate. The decrease in the measured average velocity through the orifice was in the range 70% to 56% of the theoretical value calculated using the plate displacement for various power inputs.

It was then decided to develop a numerical simulation of the formation and motion of vortex rings generated with a circular orifice plate centrally located at various elevations from the bottom, with various peripheral gaps. In a particular case the water depth to tank diameter ratios were 1.0, 1.7 and 2.77, with thermally stratified water having a relatively sharp initial density gradient, with and without a peripheral gap

around the generating plate.

Some typical computational results are presented in figures (4.10 through 4.19). The data in figures 4.11 indicate that the primary vortex ring passes upwards through the stratification interface, while a secondary vortex ring develops and travels to the bottom of the tank, where it is destroyed. It was not convenient to simulate the case of no peripheral gap around the generating plate, since the plate would in effect be attached to the wall. However, a very small gap 0.27% of the radius of the tank was investigated and considered to approach the case of no peripheral gap, some selected results of which are shown in figures 4.10 and 4.11 in different time. Figures 4.12 to 4.15 present the results of velocity vector and vorticity contour respectively for a 10 fold increase of the gap to 2.7% of the radius of the tank, which indicates the considerable effect of even a small peripheral gap on the vorticity contours (figures 4.14 and 4.15), when compared with the data presented in figure 4.11. The peripheral gap produces a line vortex which in conjunction with the wall effects creates a series of pairs of line vortices with positive and negative vorticity along the tank wall. In figure 4.14(C), it can be seen that a pair of vortices is separated from the wall and moves to the location above the primary vortex ring. These wall vortices eventually interact with the primary (and/or secondary vortex ring if the orifice plate is located in the middle level in the depth of the tank) vortex ring, as indicated in figures 4.14(D-E) and 4.15(F-H). At the beginning of this interaction, the primary vortex ring merges with the vortex with the same negative vorticity as itself in a pair of vortices which has migrated from the wall of the tank. This merged vortex ring

gradually surrounds the other vortex in the pair of vortices having the positive vorticity, and reduces its positive vorticity intensity eventually to zero. Meanwhile, the primary vortex ring is gradually elongated and extends downwards to merge with another negative vorticity wall vortex located near the generating plate, as showed in figure 4.15(G-I). This results in the considerable enlargement of the primary vortex ring with its eventual destruction. Finally, figure 4.15(I-J) shows a very large primary vortex ring which has consumed the positive vorticity wall vortex which separated from the wall in the very beginning shown in figure 4.14(C). When the peripheral gap is large and the equivalent diameter of the generator is much smaller than the vessel, the data clearly show the generation of peripheral primary and secondary linear vortex rings generated at the circumferential edge of the orifice plate as shown in figures 4.16 and 4.17. These rings are relatively weak and travel outwards in a radial direction parallel to the plate surface. Consequently, these vortex rings do not have any appreciable affect on the primary and secondary vortex rings generated at the orifice. When the ratio of the plate to orifice diameter is > 6, that is there is a considerable difference between the orifice and the plate diameter, wall or peripheral vortex rings may have little or no effect on the primary and secondary vortex rings generated at the orifice even for a small peripheral gap. The interaction between the wall or tip vortex rings and the main vortex rings can lead to enhanced mixing for relatively shallow fluid depths or stratified fluids, but might lead to poor homogeneous mixing for large fluid depths as indicated in figure 4.15. However, there will be improvement if the orifice plate is set at the middle level of fluid depth, and/or the periphery gap size is changed to an optimal value which may functionally change the vortex ring interaction distance from the orifice. The data also show that the translational velocity and vorticity intensity of a vortex ring reduces at a decreasing rate, as the peripheral gap increases until a semi-infinite flow field exists. It also confirms qualitative empirical experiments that the homogeneity of mixing can vary considerably with given fluid systems and vortex ring generators, depending on the operating conditions, such as depth of the fluid and stroke and frequency of the generator.

As described above, the peripheral primary and secondary vortex rings are relatively weak for a plate type generator with very large peripheral gap. Furthermore, peripheral tip vortices are shed in a direction from the plate towards the wall. However, when the generating plate is moved with a relatively high velocity and acceleration, it can be seen that peripheral tip vortex rings are generated in a direction parallel to the motion of the plate. That is, they move up or down from the plate periphery. These strong tip vortex rings will merge with the primary or secondary vortex rings with identical vorticity, which creates very larger vortex rings. This is seen in figures 4.18 and 4.19 which show a tip vortex ring being formed and ejected from the lower face of the plate and eventually merging with the secondary vortex ring. The resulting large vortex ring creates a considerable amount of vorticity and therefore mixing below the plate. Similarly, this will also occur above the plate.

Experiments on the generation of a single vortex ring from a centrally located orifice located near the bottom of a tank of water have been performed. Comparisons

between the experimental data and the computational results for the radius of the vortex ring "eye" and the location with respect to time, are shown in figures 4.20 and 4.21 respectively.

The computational and empirical data for the radius of a vortex ring with displacement from the generation orifice is presented on figure 4.20. It can be seen that the agreement between the computational data and the measured data are very good, except for the initial period when it is difficult to empirically measure the diameter of the vortex ring, since when a vortex ring is in the formation stages it is often not clearly defined. The agreement between the empirical and computational data for the displacement of a vortex ring with time from the generating orifice, is not so good. It can be seen that when using a coarse grid(33x85 control volumes) the computational data deviate from the measured data with an increasing magnitude, indicating a predicted much lower translational velocity than was actually being measured. It was felt that this was due to cumulative errors when using a coarse grid. Several different grid sizes were investigated but the computational time became excessive for a fine grid. The data for a medium grid size(65x167 control volumes) is also shown on Figure 4.21. It can be seen that the agreement with the empirical data is very good initially but as time progresses, above a non-dimensional time τ of about 10, the computational data notably deviates from the empirical data. In view of these observations and analysis of the computational method it is felt that the cumulative effect of "false diffusion" error is the prime suspect for the deviation of the computational data and the measured empirical data. It is also

found that a small dimensionless injecting velocity was used on the plate without considering the gap between an orifice plate and tank wall in this computational work is another reason for numerical result having deviation from experimental data.

4.5 CONCLUDING COMMENTS

Various experiments and numerical simulations have been performed for primary and secondary laminar vortex rings generated at orifices, which clearly show the importance and effects of secondary vortex rings. The numerical simulations are very useful in predicting the fluid behaviour which would be very difficult to investigate empirically with accuracy. The resulting vorticity maps are useful in predicting fluid behaviour and possible mixing phenomena in various vessel geometries. Furthermore, the numerical simulation indicates the role of secondary vortex rings, peripheral and wall vortex rings. Flow visualization has shown that the velocity-time profile of the generating device is very sensitive to and very important for the formation and transportation of vortex rings. This is very valuable when attempting to understand complicated system geometries and may provide optimal mixing conditions for various mixtures of stratified liquid/liquid or liquid/solid systems. The visualization has also shown that a primary vortex ring can actually pass through a secondary vortex ring without destruction of either ring. The value of numerical simulation of laminar vortex rings and the role of vorticity generated by wall or peripheral vortex rings, in the design of vortex ring mixers has to a large extent been established.

Numerical simulation is shown to be a very important tool when assessing the fluid flow behaviour of vortex rings in the mixing of fluids. The use of numerical simulation for large scale systems is likely to be far less costly and much more convenient than large scale experiments. It can also be used for scale-up, a very important aspect for engineering design. Currently Latto is conducting experiments and pilot scale installations in tanks of up to 400 m^3 which are not only costly but also inconvenient and time consuming. The use of numerical simulation of continuous vortex ring generation and the role of secondary vortex rings, is a very useful method for assessing the mixing effectiveness of various mixing tank and vortex ring generator geometries. For example a small peripheral gap may enhance the mixing process when the depth of the fluid is relatively shallow, whereas for a deep fluid the effects of the plate peripheral vortices are insignificant and therefore a large gap may more desirable. Furthermore, there is an indication that the primary and secondary vortex rings generated with an orifice plate can increase the mass transfer and therefore mixing almost fourfold over a tube type generator. Also the secondary vortex ring in a tube type generator can be detrimental in the generation of the primary ring, but this can be avoided if the generation motion is properly controlled.

The use of numerical simulation in conjunction with empirical data is a very important tool in the design of vortex ring generation and mixing systems using vortex ring mixing systems.

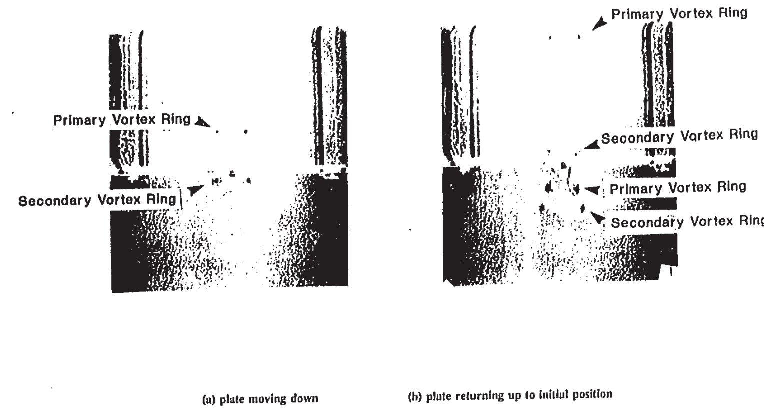

Figure 4.6. Two primary & two secondary vortex rings produced by an orifice plate for one generation cycle.

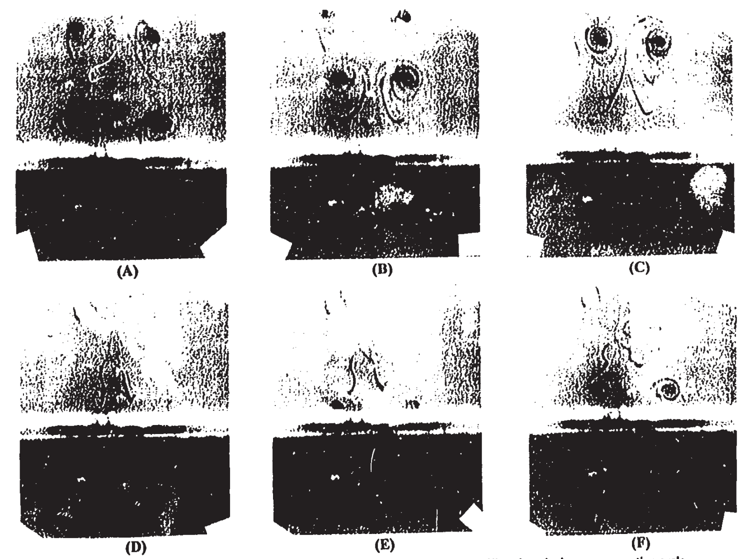

Figure 4.7 Series (A-F) of primary & secondary vortex rings produced by an orifice plate during one generation cycle.

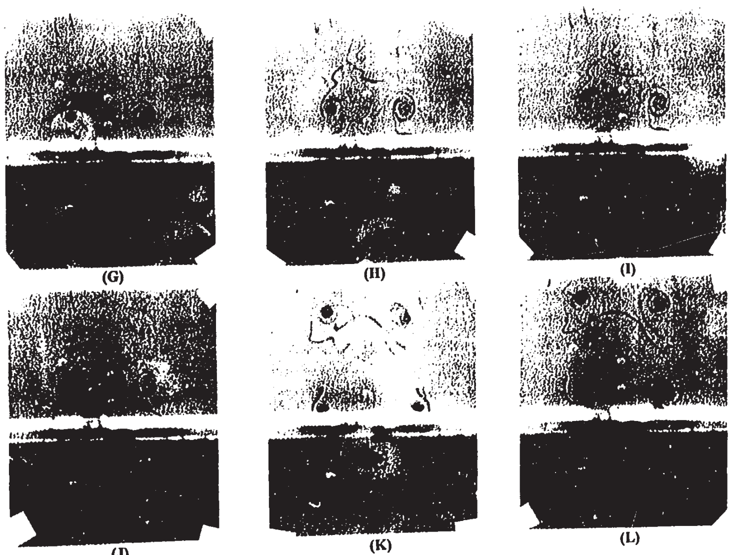

Figure 4.8 Series (G-L) of primary & secondary vortex rings produced by an orifice plate during one generation cycle.

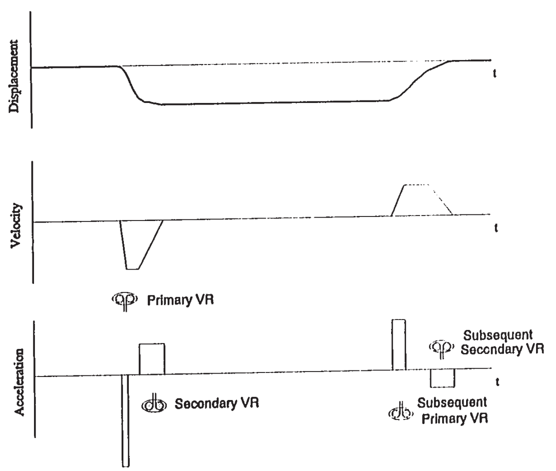

Figure 4.9 The displacement, velocity and acceleration profile of an orifice plate.

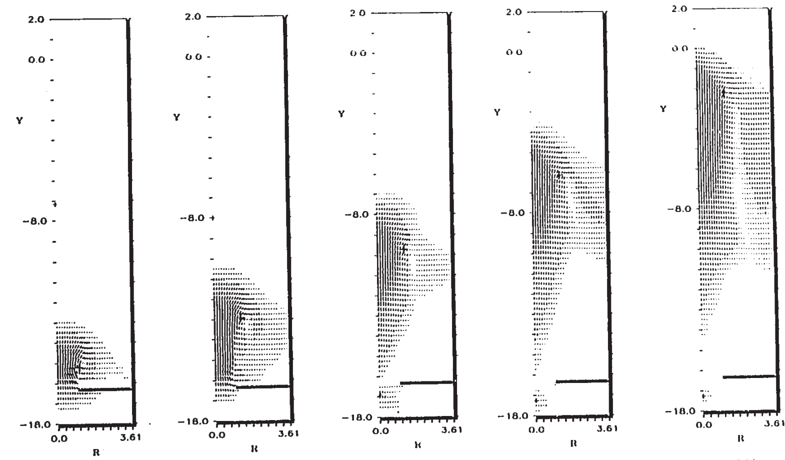

τ=2.536 τ=6.34 τ=12.68 τ=19.02 τ=25.36

Figure 4.10 Typical computer generated velocity vector plots for a plate orifice without peripheral gap, Re=17711, Ri=-0.122, Injecting time τ=6.34.

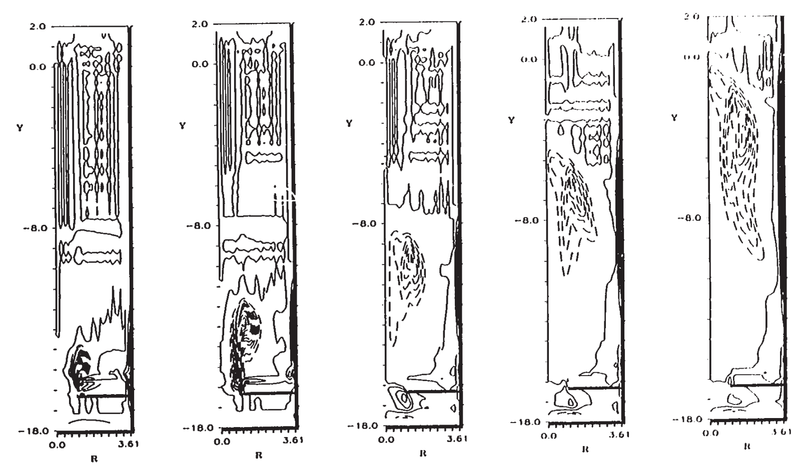

τ=2.536 τ=6.34 τ=12.68 τ=19.02 τ=25.36

Figure 4.11 Typical computer generated vorticity contour plots for a plate orifice without peripheral gap, Re=17711, Ri=-0.122, Injecting time τ=6.34.

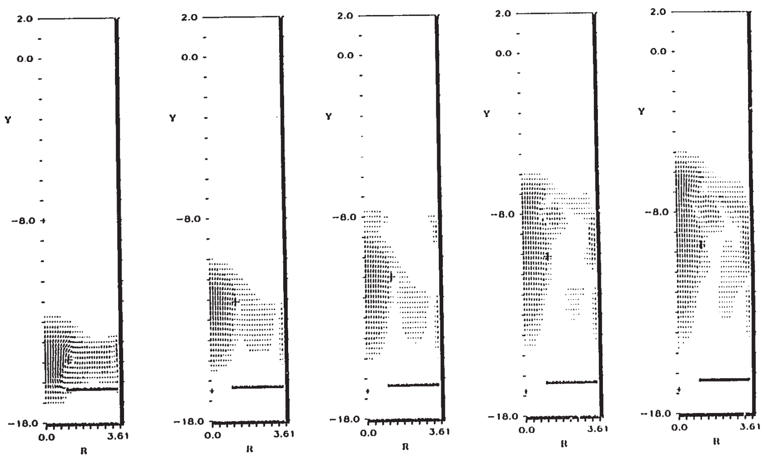

A (τ=3.76) B (τ=11.28) C (τ=15.04) D (τ=18.80) E (τ=20.304)

Figure 4.12 Typical computer generated velocity vector plots (A-E) for a plate orifice with a clearance gap of 2.7% of the tank radius, Re=10496, Ri=-0.348, Injecting time τ=3.76.

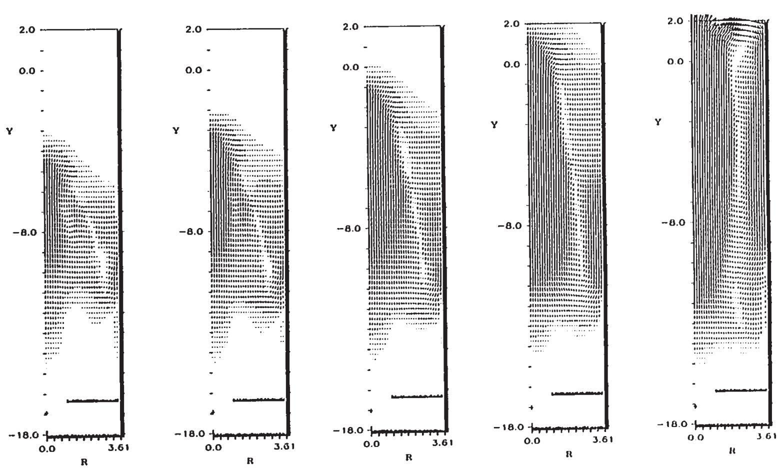

F (τ=22.56) G (τ=24.064) H (τ=26.32) I (τ=28.576) J (τ=33.84)

Figure 4.13 Typical computer generated velocity vector plots (F-J) for a plate orifice with a clearance gap of 2.7% of the tank radius, Re=10496, Ri=-0.348, Injecting time τ=3.76.

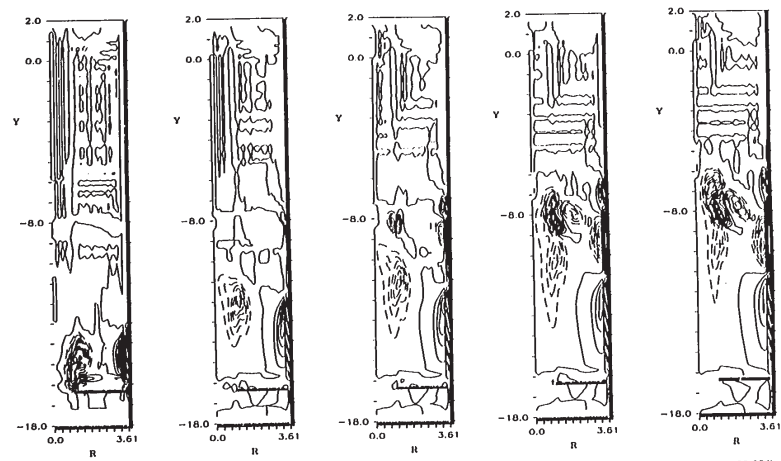

A (τ=3.76) B (τ=11.28) C (τ=15.04) D (τ=18.80) E (τ=20.304)

Figure 4.14 Typical computer generated vorticity contour plots (A-E) for a plate orifice with a clearance gap of 2.7% of the tank radius, Re=10496, Ri=-0.348, injecting time τ=3.76.

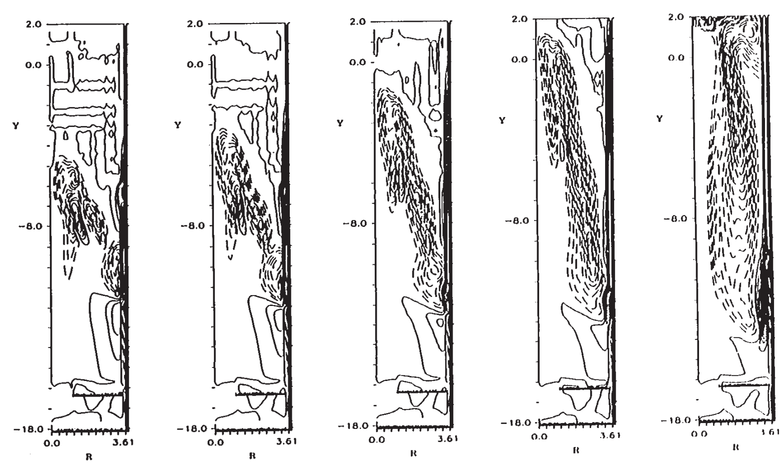

F (τ=22.56) G (τ=24.064) H (τ=26.32) I (τ=28.576) J (τ=33.84)

Figure 4.15 Typical computer generated vorticity contour plots (F-J) for a plate orifice with a clearance gap of 2.7% of the tank radius, Re=10496, Ri=-0.348, injecting time τ=3.76.

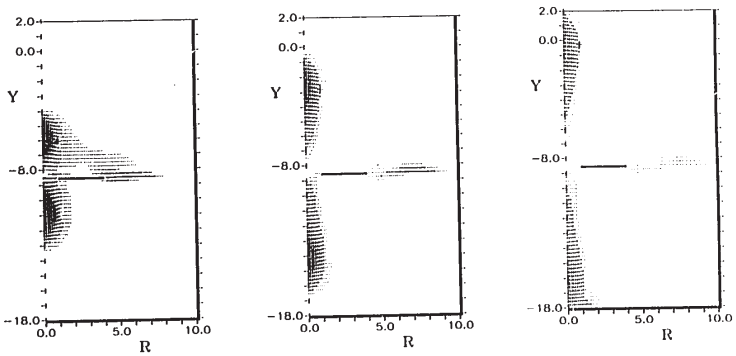

τ=3.6 τ=10 τ=16.4

Figure 4.16 A series of velocity vector plots for a orifice plate with a large peripheral gap, Re=7590 and injection time τ=0.2.

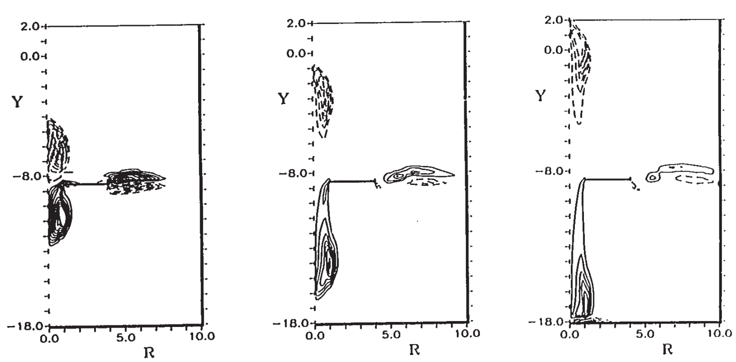

τ=3.6 τ=10 τ=16.4

Figure 4.17 A series of vorticity contour plots for an orifice plate with a large peripheral gap, Re=7590 and injecting time τ=0.2.

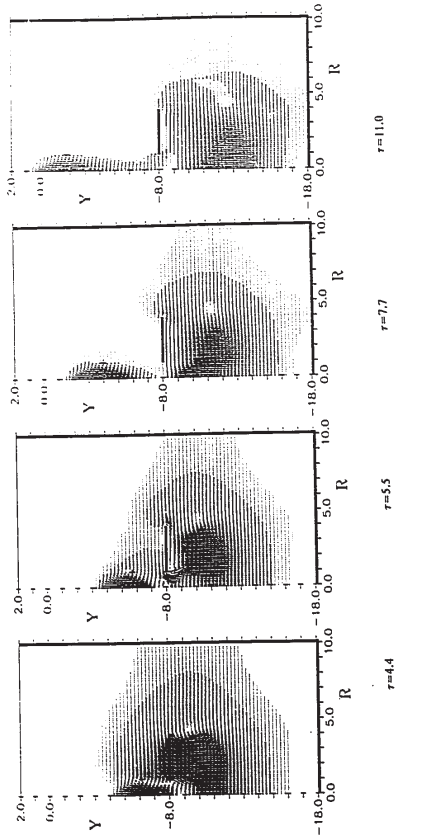

Figure 4.18 Velocity vector plots for a plate orifice with a large peripheral gap and very fast injection.

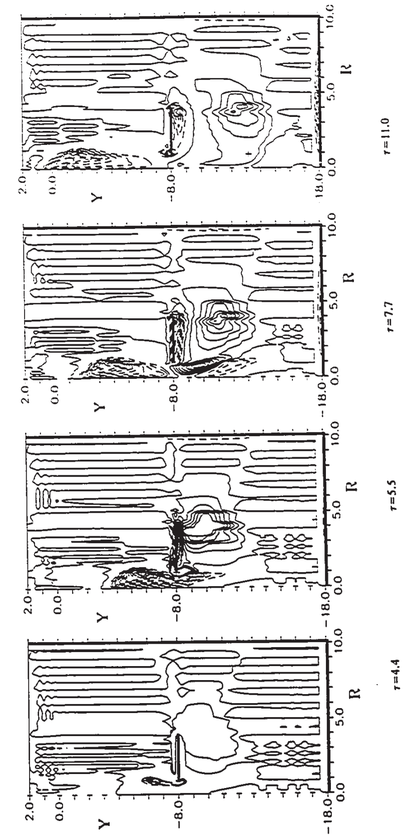

Figure 4.19 Vorticity contour plots for a plate orifice with a large peripheral gap and very fast injection.

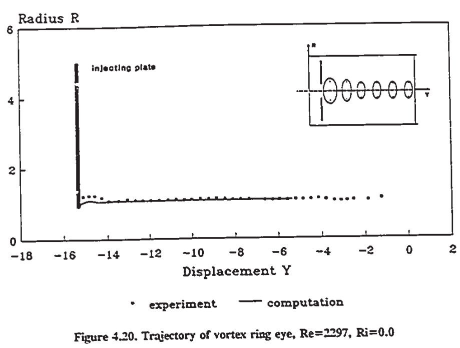

Figure 4.20. Trajectory of vortex ring eye, Re=2297, Ri=0.0

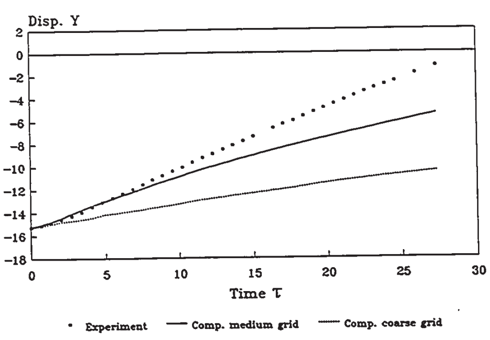

Figure 4.21. Displacement of vortex ring vs. time, Re=2297, Ri=0.0

CHAPTER 5

NUMERICAL SIMULATION OF VORTEX RINGS PENETRATING A STRATIFIED NON-NEWTONIAN FLUID

5.1 INTRODUCTION

The dynamics of vortex rings has been studied theoretically and empirically for a long time. However, virtually all of the studies are limited to Newtonian fluids. A notable amount of the numerical simulation research has been devoted various aspects of non-Newtonian fluid mechanics, but none of the studies appear to address the behaviour of vortex rings in non-Newtonian fluids. This is understandable in view of the lack of interest in the application of vortex rings for specific purposes. Recently, Latto (1987)(1989)(1990)(1991)(1992) has developed equipment which generate vortex rings for the agitation and mixing of a wide range of fluids. Many practical applications of these type of mixers involved in the agitation of liquids and slurries which exhibit non-Newtonian behaviour.

Empirical experiments with non-Newtonian fluids and slurries conducted by Latto have indicated that the vortex ring mixers give remarkably good mixing. However it is to some extent difficult to predict the performance characteristics of a vortex ring mixer under these circumstances. Furthermore, Latto has at times observed unpredictable mixing behaviour, especially when non-Newtonian shear thinning or shear thickening slurries were involved. It is difficult to measure or observe localized flow behaviour in the majority of non-Newtonian liquids or slurries due to the fact that they are opaque or have particles in suspension. Numerical simulation and the development of computer codes have considerable value in the prediction and understanding of the behaviour of vortex rings and consequently could have a considerable value in the design of vortex ring mixing systems involving non-Newtonian fluids.

Numerical methods for non-Newtonian flow have considerably progressed since the late 1970's. Much has happened in that field since a review by Crochet and Walters (1983) and a monograph by Crochet, Danies and Walters (1984), which gave a snapshot of the numerical landscape in rheology. Later, Keunings (1987) published a comprehensive review on numerical simulation in non-Newtonian fluids.

Most of the previous papers which studied the numerical solution of the two dimensional Navier-Stokes equations for non-Newtonian fluids adopted stream function/vorticity finite difference or finite element methods. In contrast, the present study of the numerical simulation considers a method which combines the finite difference method (modified Patankar's SIMPLER method) and the necessary iterative

techniques to solve the axi-symmetric flow problem of injecting vortex rings into a tank with power law fluids, from a tube generator centrally located near the free surface including buoyancy.

5.2 STUDY AND FORMULATION OF THE PROBLEM

In order to simulate the formation and behaviour of vortex rings generated at orifices, a numerical solution using a control-volume based finite-difference technique (Patankar's SIMPLER technique (1980)) was employed to solve the continuity, Navier-Stokes and energy equations simultaneously in cylindrical coordinates r(r,0,y) and the corresponding vector field v=(u.0,v). This technique employed a control-volume approach to discretize the governing equations. The velocity control-volumes were staggered with respect to the control-volumes for the pressure and temperature. The fluid was incompressible, with constant properties. The solution was assumed to be axi-symmetric laminar, and the liquid is presented by a power law model described by Bird (1960, 1977). The Boussinesq approximation was employed for the buoyancy term in Y direction momentum equation of equation (7). These governing equations are as follows:

CONSTITUTIVE EQUATION:

$$\tau=-m|\pi/2|^{(n-1)/2}\Delta \tag{4}$$

where in cylindrical coordinates the second invariant of the rate of deformation tensor, π, can be expressed as

$$\pi=\Delta.\Delta=4(\frac{\partial u}{\partial r})^2+4(\frac{u}{r})^2+4(\frac{\partial v}{\partial y})^2+2(\frac{\partial u}{\partial y}+\frac{\partial v}{\partial r})^2 \tag{5}$$

The other governing equations are

CONTINUITY EQUATION:

$$\frac{1}{r}\frac{\partial}{\partial r}(ru)+\frac{\partial v}{\partial y}=0 \tag{6}$$

MOMENTUM EQUATION:

$$\begin{aligned}&\rho(\frac{\partial u}{\partial t}+u\frac{\partial u}{\partial r}+v\frac{\partial u}{\partial y})=-\frac{\partial p}{\partial r}-[\frac{1}{r}\frac{\partial}{\partial r}(r\tau_{rr})-\frac{\tau_{\theta\theta}}{r}+\frac{\partial\tau_{ry}}{\partial y}]\\&\rho(\frac{\partial v}{\partial t}+u\frac{\partial v}{\partial r}+v\frac{\partial v}{\partial y})=-\frac{\partial p}{\partial y}-[\frac{1}{r}\frac{\partial}{\partial r}(r\tau_{ry})+\frac{\partial\tau_{yy}}{\partial y}]+\rho g\end{aligned} \tag{7}$$

ENERGY EQUATION:

$$\rho C_p(\frac{\partial T}{\partial t}+\frac{\partial T}{\partial r}+\frac{\partial T}{\partial y})=k[\frac{1}{r}\frac{\partial}{\partial r}(r\frac{\partial T}{\partial r})+\frac{\partial^2 T}{\partial y^2})] \tag{8}$$

The variables are non-dimensionalized as follows:

$$R=\frac{r}{r_i},\quad Y=\frac{y}{r_i},\quad U=\frac{u}{-v_*},\quad V=\frac{v}{-v_*},$$

$$Pr=\frac{\mu C_p}{k},\quad Re=\frac{\rho r_i^n}{m(-v_*)^{n-2}},\quad \sigma_{ij}=\tau_{ij}(\frac{r_i}{-v_*})^n\frac{1}{m},$$

$$\theta=\frac{T-T_2}{T_1-T_2},\quad P=\frac{p-p_0}{\rho v_*^2},\quad \tau=\frac{t(-v_*)}{r_i},$$

where v_*, r_i are a reference velocity and the inlet tube radius respectively.

Finally, the governing non-dimensionalized equations for axi-symmetric injecting flow in a tank may be written as following

$$\begin{aligned}&\frac{1}{R}\frac{\partial}{\partial R}(RU)+\frac{\partial V}{\partial Y}=0\\&\frac{\partial U}{\partial\tau}+U\frac{\partial U}{\partial R}+V\frac{\partial U}{\partial Y}=-\frac{\partial P}{\partial R}-\frac{1}{Re}[\frac{1}{R}\frac{\partial}{\partial R}(R\sigma_{rr})-\frac{\sigma_{\theta\theta}}{R}+\frac{\partial\sigma_{ry}}{\partial Y}]\\&\frac{\partial V}{\partial\tau}+U\frac{\partial V}{\partial R}+V\frac{\partial V}{\partial Y}=-\frac{\partial P}{\partial Y}-\frac{1}{Re}[\frac{1}{R}\frac{\partial}{\partial R}(R\sigma_{ry})+\frac{\partial\sigma_{yy}}{\partial Y}]+Ri\theta\\&\frac{\partial\theta}{\partial\tau}+U\frac{\partial\theta}{\partial R}+V\frac{\partial\theta}{\partial Y}=\frac{1}{PrRe}[\frac{1}{R}\frac{\partial}{\partial R}(R\frac{\partial\theta}{\partial R})+\frac{\partial^2\theta}{\partial Y^2}].\end{aligned} \tag{10}$$

An important parameter is the dimensionless injection time. which is a measure of the volume of fluid injected through the generating tube into the tank. An optimal value of $\tau_{in}=5.5$ was used, which was based on experiments by Baird (1979) and Latto (1987, 1989).

The velocity boundary condition for the fluid surface outside of the inlet tube is as follows: no shear stress ($\partial U/\partial Y=0$), and $V_{out}=-V_{in}*r_i^2/(r_o^2-r_i^2)$, and all of the solid boundaries are assumed adiabatic.

In order to facilitate the solution of the problem, it was attacked from a different standpoint from that which was previously employed by others, and author chose to regard the system of governing equations as composed of two components. Firstly, the equations for the velocity, pressure and temperature were time-marched, and secondly the computations repeated for the new stress components σ_{rr}, $\sigma_{\Theta\Theta}$, σ_{ry}, σ_{yy} from the updated velocity vector, and then for the new velocity components U, V from the updated stress tensor in an iteration process.

The simulation considered a cylindrical tank system which initially contained a stationary fluid, as depicted in figure 3.3(a). The fluid in the tank was considered to be initially stably stratified, having a higher density in the lower half than the upper half, with a sharp density interface at the middle height.

The formation of a vortex ring was simulated numerically by rapidly injecting a quantity of the lower density fluid through a generator tube. The generator tube has its axis normal to the liquid surface and symmetrical to the tank, and its open end below the liquid surface. The tube radius was one unit with the plane of its opening 2 units below the fluid free surface. A tank radius of 10 units and a liquid depth of 20 units was considered. In order to investigate the numerical simulation, a typical fluid having a 4% paper pulp in water was initially considered, having a power law index n = 0.571, and a Prandtl number of 7.0.

The velocity distribution of the fluid in the generator tube during the generation of a vortex ring, was assumed to be radially uniform in a plane at the level of the fluid free surface, i.e. Y=2. This radially uniform velocity distribution was then varied with time, as indicated in figure 3.4. A reference velocity v_*, which is defined as the time

averaged fluid injection velocity in the generator tube over the injection period, i.e. $0 \leq t \leq t_{in}$, and $v_{in}=0$ for the time period $\tau \geq \tau_{in}$ was used.

During the injection/generation phase, the vorticity near the exit of the generator tube is high. When the fluid injection is terminated, a fully developed vortex ring will normally be formed, provided it complies with the deductions of Latto (1987) and/or Baird et al(1977) i.e. $0.5 \leq \tau_{in} \leq 3.8$. The vortex ring thus formed will travel away from the tube as depicted in figure 1.1. Furthermore during the travel of a vortex ring, some fluid originally contained in the ring is discharged in the tail or wake behind the ring, also shown in figure 1.1.

5.3 RESULT AND DISCUSSION

Various fluids were investigated. Some typical cases of an injecting Reynolds number Re of 10,000 and injection time τ_{in}=5.5 was used to evaluate the computational procedure. Solutions were obtained for power law indexes 'n' of 0.17, 0.571, 1.50 and Richardson numbers Ri of 0.0, 0.01, 0.1, for time interval in the range 0 to 20 τ_{in}. Obviously the buoyancy effect is negligible when Ri = 0.0.

Generally, it is apparent that the formation, traversing motion and dissipation of a laminar vortex ring in non-Newtonian fluids are basically the same as those for a laminar vortex ring in Newtonian fluids obtained by Papple and Latto (1991), i.e. a

power law index n = 1.0. At the end of the injection stage, a full vortex ring has formed adjacent to the outlet of a tube, and the radius ratio of vortex ring eye and tube is about 1.5. The vortex ring then travels away from the orifice to penetrate the density interface with a small increase in the radius of the vortex ring eye and a gradual decrease its forward velocity and vorticity. When a vortex ring contacts the bottom of tank(solid boundary), i.e. τ is slightly greater than $12\tau_{in}$, it dissipates and expands radially at the solid boundary. This dissipative (destruction) stage results in mixing of the different density fluids. Typical plots of velocity vector fields, vorticity contours and temperature field isotherm plots, at various times for a fluid having a power law index n of 0.17 are shown in figures 5.1, 5.2 and 5.3 respectively. Figures 5.4 and 5.5 are plots of velocity vector fields and vorticity contours of a vortex ring for power law fluids with an index n = 0.571, while figures 5.6 and 5.7 are for power law index n of 1.5.

It is obvious from the computational data that when Ri and Re are constant the vortex ring trajectories are basically the same, even when the power law indexes n are 0.17, 0.571, 1.0 and 1.5, as shown in figure 5.8.

From flow visualization it is apparent that the fluid in a vortex ring rotates with respect to its ring eye (the location of maximum vorticity) while it moves forward. This motion results in the vortex ring in effect rolling through the ambient fluid, similar to a wheel rolling along a solid surface. It is this rolling motion that results in very low drag (both skin drag and form drag) on the vortex ring and produces low shear rate (dv/dr)

on the ring surface. This can result in a relatively long travelling distance for a vortex ring before it destructs.

The rate dv/dr in most regions of a laminar vortex ring is relatively low and approximately zero at the vortex ring side periphery. Consequently, it can be expected that the type of power law fluids (different power law index n) will have very little effect on the trajectory of a vortex ring. The shear stress for each value of n is similar & quite small at the outer surface of a vortex ring. It is for this reason that there is good agreement between the data for the vortex ring trajectories in all cases and that it does not depend on the power law index n and fluid viscosity η.

For non-Newtonian fluid density stratification where buoyancy is significant, vortex rings behave in a similar manner as in Newtonian fluids, as indicated by the curves of the trajectories of the eye of the rings curves, figure 5.10. When Ri=0.01, after penetrating the interface, the vortex ring decreases in radius. The vortex ring penetrates the high density fluid to about the tank bottom before losing its downward momentum. Some of the fluid originally contained in the ring exits through the tail, then rises because of buoyancy. When the vortex ring hits the bottom then rebounds, its energy losses are high. The fluid within the ring continues to rotate although the vortex ring is no longer moving downward. The vortex ring then rapidly dies out.

The trajectories for Ri≥0.1 (figure 5.10) are distinctly different from those for

$Ri \leq 0.01$ in that the lower density vortex ring does not penetrate very far into the higher density fluid. The ring only slightly penetrates under these conditions, and then rebounds back toward the interface. This has been observed in numerous experiments with dyed vortex rings in hot/cold water, saline/water, diluted corn syrup/water, and isoper/water stratified systems. The energy losses are relatively significant, since the fluid in the vortex ring rotates and basically self destructs at the liquid/liquid interface. This in actual fact, causes some interfacial mixing and produces a third layer. This continuous destruction of vortex rings at the density interface eventually permits progressively more penetration of vortex rings and can result in total penetration of the vortex rings into the higher density fluid, without any appreciable increase of the Richardson number of the generated vortex ring. This is because for a given generating velocity, the Richardson number of the vortex ring in the diluted third layer is reduced due to the reduction in the local ambient density in the third layer. Thus as a vortex ring destructs after passing through the intermediate layer, the thickness of the intermediate layer increases. The process continues until the intermediate layer becomes the second layer and homogeneity of the fluids rapidly progresses.

An important aspect of the computer simulation is that it is possible to generate vorticity and flow patterns within a fluid field. This is of considerable value for assessing flow behaviour and design criteria for mixing systems. For example it has been found from the computer simulations that secondary vortex rings may have either a beneficial or a harmful effect on mixing for various mixing system geometries. The effects were

qualitatively observed but not understood until the computer simulation was performed. It is also quite difficult and expensive to perform the majority of mixing investigations for many liquids and slurries, and mixing system geometries. Often computational simulation can be done with much greater ease and lower costs than by empirical experiments, such as flow visualisation or anemometry. The turbidity and nature of slurries would make these type of experiments virtually impossible.

5.4 CONCLUDING COMMENTS

Numerical simulation of the generation and propagation of vortex rings in non-Newtonian fluids has been done. The resulting data and graphical presentations of vorticity, temperature and velocity maps clearly show the value of this technique for such a complex process and phenomena. It was and is difficult to quantitatively confirm the information thus obtained, but the value of the numerical results indicates the possible interaction between vortex rings, and vortex rings and vorticity generated due to solid bodies such as walls and solid boundaries. It is relatively difficult to perform numerous experiments to assess the correct configuration of a mixer and the mixing vessel or system. The numerical approach is of considerable value in assessing the optimal configuration.

When comparing a laminar vortex ring's trajectory for various power law non-Newtonian fluids, the major difference between them is shear thinning ($n < 1.0$) and

shear thickening ($n > 1.0$) fluids, as shown by vorticity contours in figure 5.9. Although a vortex ring has basically the same location and vorticity intensity after a period of 4 τ_m in shear thinning and shear thickening fluids, for shear thinning fluid there is notable motion and vorticity created in the central column and near the bottom of tank in a region where a vortex ring has not reached. However nothing happens in comparable regions for shear thickening fluids. Obviously, shear stress really plays an important role in the agitation of fluids using this technique. It is quite apparent from the numerical data that the vorticity and disturbance at locations distant from generation location is much more evident with power law shear thinning fluids than power law shear thickening fluids. This is useful when designing vortex ring mixing systems for various non-Newtonian power law fluids. It is also evident from this data that faster mixing will most likely occur in shear thinning fluids than shear thickening fluids, which we have observed in qualitative experiments with slurries such as, aqueous MgOH and $CaCO_3$ suspensions.

It is also of interest to note that the numerical analysis clearly shows the effects of power law fluids on the behaviour of laminar vortex rings appear to be limited to far field vorticity, and that the trajectory of a vortex ring is not appreciably affected by the type of power law fluid.

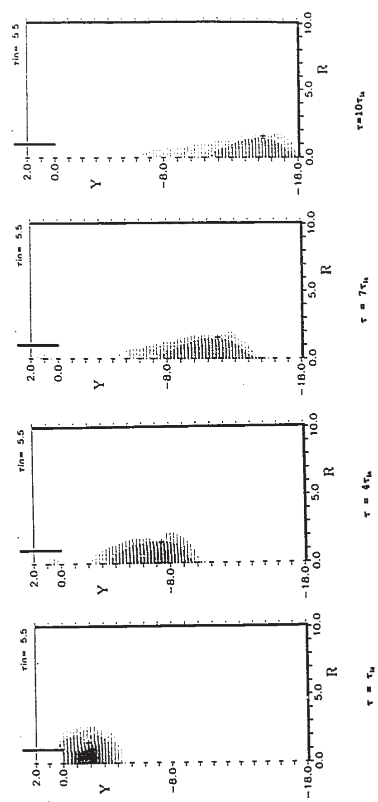

Figure 5.1 Velocity vector plots of a vortex ring for Re=10000, n=0.17.

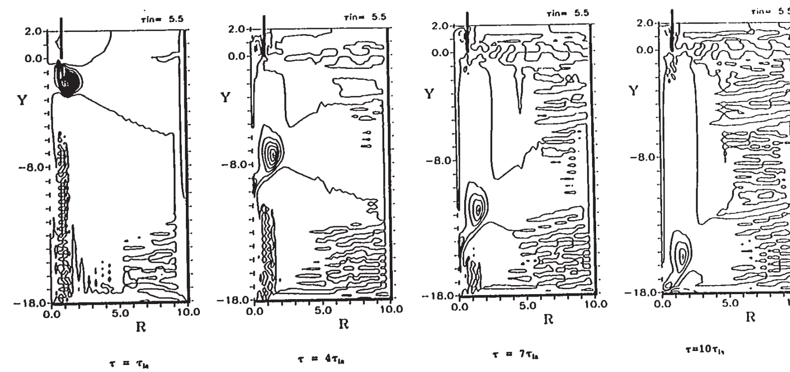

Figure 5.2 Vorticity contour plots of a vortex ring for Re=10000, n=0.17.

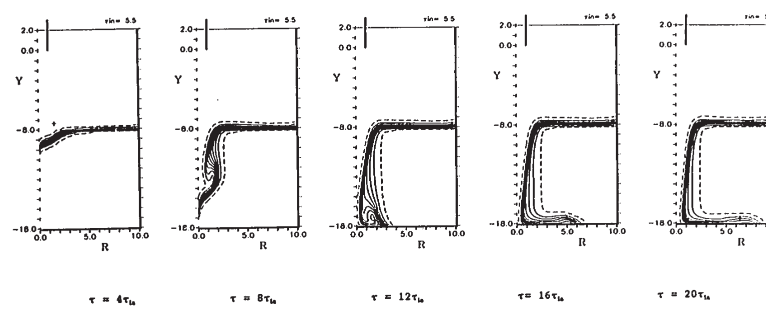

Figure 5.3 Temperature field plot for Re=10000, Ri=0.00, r_{in}=5.5 n=0.17. (isotherms every 10%, dashed lines indicate Θ=0.01 and 0.99; the + indicates the vortex ring eye location)

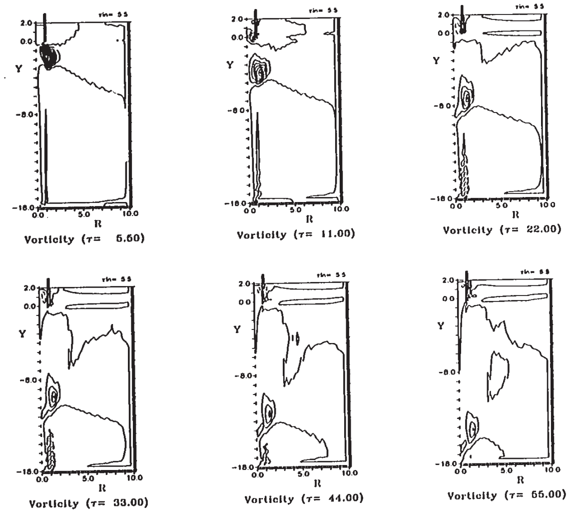

Figure 5.4 Vorticity contour plots for a vortex ring when Re=10000, n=0.571.

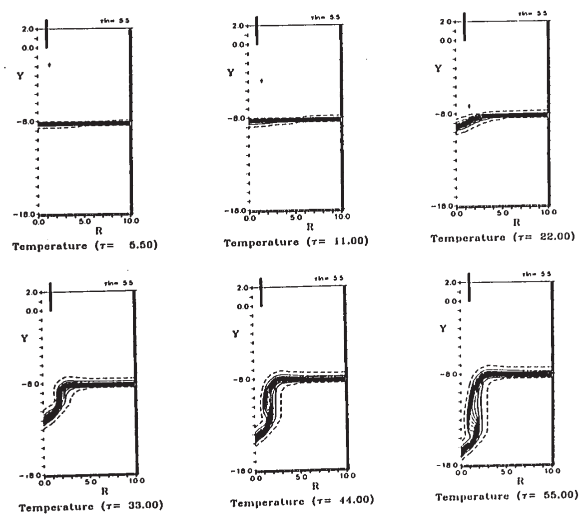

Figure 5.5 Temperature field plot for Re=10000, Ri=0.00, r_{in}=5.5 n=0.571. (isotherms every 10%, dashed lines indicate Θ=0.01 and 0.99; the + indicates the vortex ring eye location)

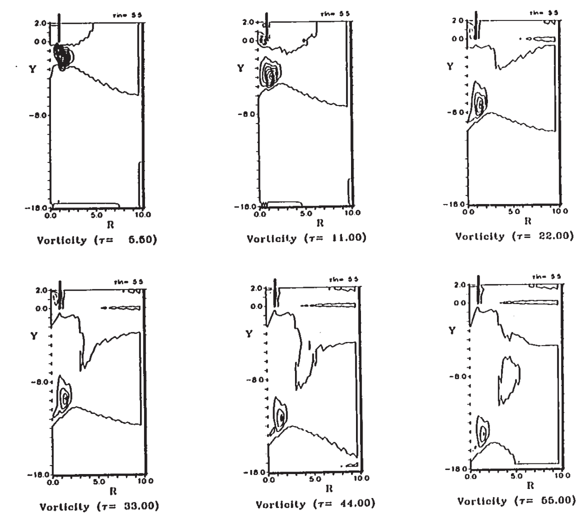

Figure 5.6 Vorticity contour plots for a vortex ring when Re=10000, n=1.5.

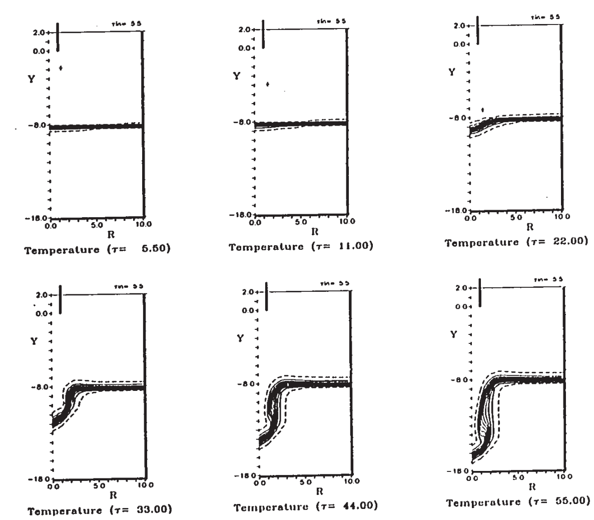

Figure 5.7 Temperature field plots for Re=10000, Ri=0.00, τ_{in}=5.5 n=1.5. (isotherms every 10%, dashed lines indicate Θ=0.01 and 0.99; the + indicates the vortex ring eye location)

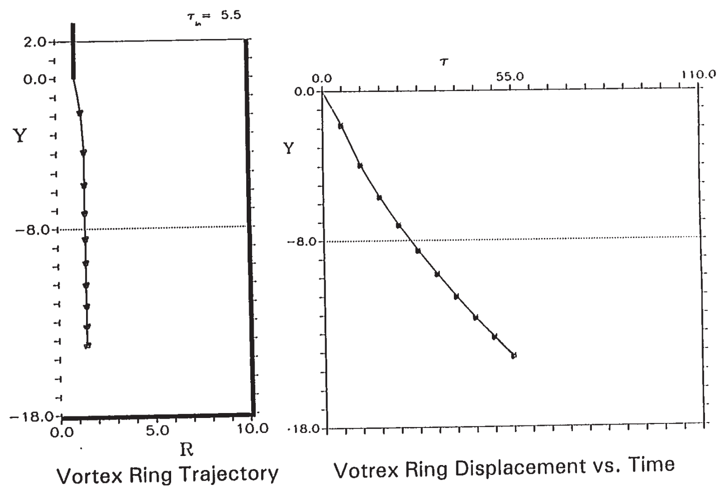

Re=10000, Ri=0.0

Figure 5.8 A comparison of vortex ring trajectory & vortex ring displacement vs time for Newtonian fluid (x:n=1) and power law model fluids (▽:n=0.17, O:n=0.571, □:n=1.5).

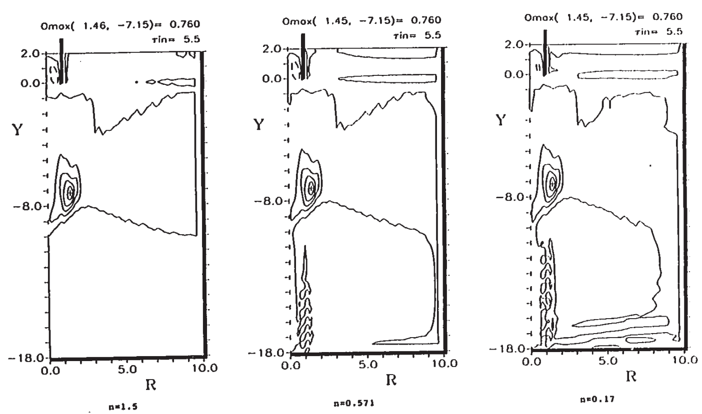

Re=10000, Ri=0.0

Figure 5.9 Typical computer generated vorticity contour for a vortex ring ejected from a tube, shear thinning (n<1) and shear thickening fluids (n>1), after four times the injection time, indicating far reaching effects of vortex ring. (Re=10000, Ri=0.0)

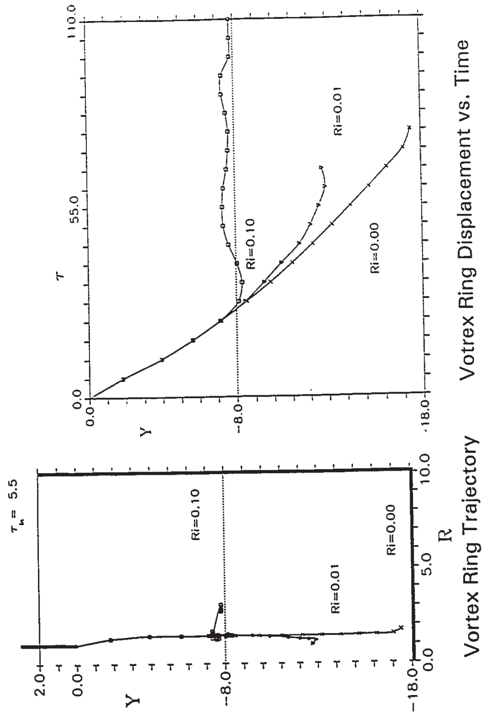

Figure 5.10 Effect of Richardson number on vortex ring's penetration through a stratified fluid interface for a power law model fluid (n=0.571). Re=10000; x:Ri=0.0, ∇:Ri=0.01, ○:Ri=0.1.

CONCLUSIONS

It is apparent from the literature that prior research has concentrated on theoretical and fundamental aspects of vortex rings, with very little work on the applied aspects of vortex rings. In view of this, this research program was directed at a theoretical and practical understanding of the behaviour of vortex rings under realistic and complex conditions. The formation of laminar vortex rings was numerically simulated, using a control volume based finite difference method, by considering the ejection of a quantity of fluid through a tube centrally located near a free surface, or an orifice plate generator located at various horizontal levels in a tank. Initially, a stably stratified fluid was considered. Buoyancy effects are also included in the computational work, which was not the case for prior reported work. Furthermore flow visualization and empirical measurements have been preformed to validate the numerical work.

Of interest was the application of vortex rings for the mixing of the fluids. In order to do this several computer models have been developed for the numerical simulation of laminar vortex rings such as the behaviour in stratified Newtonian & non-Newtonian fluids; the penetration of vortex ring through an interface; the interaction between adjacent vortex rings such as wall vortex rings; and formation and motion of a secondary vortex injected from an orifice. Under particular conditions, experiments have

been performed to study the behaviour of the laminar vortex rings, such as vortex rings encountering a density interface; vortex ring formation, transportation, transition and turbulent decay; sensitivity and dependence of vortex rings on the injecting motion or velocity.

Notable contribution have been made in this research program. The numerical results and experiment data showed that:

(1) The penetration and trajectory of a laminar vortex ring through a density gradient are virtually independent of the defined injection Reynolds number, but primarily dependent on the Richardson number. A large Ri, (when $Ri > 0.1$), represents a large positive or negative buoyancy force, which resists the vortex ring penetrating an interface and forces it back to the original fluid layer in which it was formed. A $Ri < 0.1$ will result in the penetration of a vortex ring through the density stratified interface. Basically Ri is a function of the average injection velocity for a given stratified fluid system and a given vortex ring generation device. For a large Ri, usually it is practical and reasonable to increase the injection or generation velocity or to employ a smaller diameter tube or orifice for a given stratified fluid system to decrease the Ri. The injection velocity profile and injecting frequency of a vortex ring has strong effects on its mixing behaviour. There appears to be an optimal value of injecting velocity or frequency for the effective mixing in a particular case.

(2) Laminar vortex rings in a power law fluids behave inviscidly, and virtually the same as in Newtonian fluids for a certain range of injecting Reynolds numbers. This can be understood because the shear rate is very small at the periphery of a vortex ring when it passes through a non-Newtonian fluid and consequently neither the index 'n' (including n=1 for Newtonian fluid) nor the viscosity have any notable effects on the degree of shear stress. However the viscosity model does have an effect in the generation stage. Although the trajectories and velocity of a vortex ring are basically the same for non-Newtonian and Newtonian fluids after a certain injection time, for shear thinning fluids notably more motion and vorticity are created in the central column and at locations remote from the generating orifice and the actual vortex ring, when compared with shear thickening fluids.

(3) Secondary vortex rings generated at an orifice have approximately similar trajectories and vorticity intensities to those of primary vortex rings, if a trapezoidal injection velocity profile is adopted, except that they travel in an opposite directions. This can result in a fourfold mass transportation and therefore almost fourfold mixing compared with a tube type generator. It is also indicated that the secondary vortex ring in a tube type generator can be detrimental in the generation of the primary ring.

(4) Localized vorticity with various intensity, such as wall vortex rings generated at a peripheral gap between plate and tank wall, or tip primary and secondary vortex rings generated at an orifice plate periphery, may have different interactions with the primary

and secondary vortex rings depending on the gap size, injecting intensity etc. This phenomenon has not been described before and appears to be of considerable interest for both fundamental and mixing studies. For a small peripheral gap, the wall vortex rings are gradually consumed by the primary and secondary vortex rings resulting in their enlargement and an increase in their vorticity intensity. There is no doubt that adjusting the size of the peripheral gap may affect the distance from the orifice plate for the wall vortex rings separating from the vessel wall, and therefore control the fluid mixing. When the gap size is increased to a large enough value, only weak tip vortex rings travel in the horizontal direction towards the vessel wall. There is no interactions between them and the primary & secondary vortex rings. If the orifice plate has a strong down stroke with high velocity and acceleration a strong tip vortex ring leaves the plate periphery and travels parallel to the motion of the plate. This tip vortex ring merges with the secondary vortex ring with identical vorticity and becomes a large vortex ring.

(5) The velocity and behaviour of vortex rings are very dependent on the displacement-time motion profile of the generating device. Different displacement-time profiles will produce different generation velocity and acceleration profiles, which will profoundly affect the properties of the primary and secondary vortex rings, such as their motions, velocities, vorticities, sizes and the interaction of these two types of rings. These various changes in the properties of the primary and secondary vortex rings definitely may make possibly flexible operation of a mixer and satisfy the requirements of special mixing systems e.g. sedimentary slurries, suspension of slurries. Thus by having a knowledge

of the behaviour of vortex rings with respect to motion of the generating device, an intelligent interactive mixer design may be possible.

Several experiments on vortex rings injected from a tube type generator and an orifice type generator have been performed, and the comparison between experiment data and numerical results has also been made. It shows that the numerical modelling of the laminar vortex ring behaviour is relatively good. The computer Finite Difference (CFD) technique is becoming increasingly popular as a tool for some very good reasons. CFD numerical simulation gives a complete picture of the flow regime, which is not normally available from experimental measurements, such as wall vortex rings and their interaction with the primary and secondary vortex rings. Since they do not involve real plant systems and fluids, CFD numerical models are often cheaper, safer and more convenient to run than their physical equivalents, and once a model has been set up it is easy to make changes and run "what if?" queries for various parameter changes.

REFERENCES

Anon, 1970, "Vortical Chimneys", Nature, Vol. 226, pp. 584.

Baird, M. H. I., Wairegi, T. and Loo, H. J., 1977, "Velocity and Momentum of Vortex Rings in Relation to Formation Parameters", The Canadian J. of Chemical Engineering, Vol. 55, pp. 19-26.

Baird, M. H. I., Rama Rao, N. V. and Latto, B., 1992, "Liquid-Liquid Extraction Using Vortex Rings in A Batch Cell", Trans. Inst. Chem. Eng., Vol. 70, Part A, pp. 323-332.

Bird, R. B., Armstrong, R. C. and Hassager, 0., 1977, "Dynamics of Polymeric Liquids: vol. 1 Fluid Mechanics, John Wiley and Sons.

Bird, R. B., Stewart, W. E. and Lightfoot, E. N., 1960, "Transport Phenomena, John Wiley and Sons, New York. London.

Brasseur, J. G., 1986, "Evolution Characteristics of Vortex Rings Over a Wide Range of Reynolds Numbers", AIAA/ASME 4th Fluid Mechanics, Plasma Dynamics and Lasers Conference, AIAA-86-1097.

Busnaina, A. A. and Lilley, D. G., 1983, "Computer Prediction of Local Destratification Near Low-Level Release Structures of Reservoirs", Journal of Fluid Engineering, Vol. 105, pp. 65-71.

Chandrasekhar, S., 1961, "Hydrodynamic and Hydromagnetic Stability", Oxford, london, pp. 16-17.

Crochet, M. J., Davies, A. R. and Walters, K., 1984, "Numerical Simulation of Non-Newtonian Flow", Elsevier, Amsterdam.

Crochet, M. J. and Walters, k., 1983, "Numerical Methods in Non-Newtonian fluid", Mechanics, Ann. Rev. Fluid Mech., Vol. 15, pp. 241-260.

Dahm, W. J. A., Scheil, C. M. and Tryggvason, G., 1989, "Dynamics of Interaction with A Density Interface", J. Fluid Mech., Vol. 205, pp. 1-43.

Didden, N., 1977, Ph.D. Dissertation, University of Gottingen.

Didden, N., 1979, "On the Formation of Vortex Rings: Rolling and Production of Circulation", J. Appl. Math. Phys., Vol. 30, pp. 101-116.

Friebel, W. C. and Rath, H. J., 1987, "The Formation and Behaviour of Laminar Vortex

Rings", PHOENICS Users Conference, #1987/56.

Glezer, A., 1988, "The Formation of Vortex Rings", Phys. Fluids, Vol. 31, No. 12, pp. 3532-3542.

Ho, S.K., 1991, "An Experimental and Numerical Study of the Effects of Surrounding Disturbances on Vortex Rings", M.Eng. Thesis, McMaster University.

Honji, H. and Tatsuno, M., 1976, "Vortex Rings in a Stratified Fluid", J. Phys. Soc. Japan Vol. 41, No. 6, pp. 2121-2125.

Hecht, A. M., Bilanin, A. J., Hirsh J. E. and Snedeker, R. S.,1980, "Turbulent Vortices in Stratified Fluids, AIAA Journal, Vol. 18, No. 7, pp. 738-746.

Irdmusa, J. Z. and Garris, C. A., 1987, "Influence of Initial and Boundary Conditions on Vortex Ring Development", AIAA J. Vol. 25, No. 3, pp. 371-372.

Johnson, V. E. et al, 1982, "Cavitating and Structured Jets for Mechanical Bits to Increase Drilling Rate", ASME-Paper 82-Pet-13.

Kendig, F., 1972, "The Science of Smoke Rings and Doughnuts", Saturday Review, March 18, pp. 40-44.

Keunings, R., 1987, "Simulation of Viscoelastic Fluid Flow", to appear in C.L. Tucker (Ed), Fundamentals of Computer Modelling for Polymer Processing, Carl. Hanser Verlog.

Latto, B., 1987, "New Mixer for Slurries and Stratified Fluids", 12th Int. Conf. on Slurry Technology, Mar/April.

Latto, B., 1989, "Novel Vortex Ring Mixers for Slurries and Stratified Liquids, 14th Int. Conf. on Coal & Slurry Technology, April.

Latto, B. and Shoukri, M., 1990, "Use of Vortex Rings for Mixing", Industrial Application of Fluid Mechanics, FED Vol. 100, ASME, Eds. Sherif, Morrow, Marshall and Dalton.

Latto, B., Papple, M. L. C., Shoukri, B. and Baird, M. H. I., 1990, "Mixing of a Thermally Stratified Fluid by Injecting a Series of Vortex Rings - A Numerical Simulation", Trans IChemE, Vol. 68, Part A, pp. 457-463.

Latto, B., 1992, "Vortex Ring Mixers for Slurries and Controlled Addition of Gases and Liquids", Proc. 19th Int. Conf. on Coal and Slurry Tech.

Latto, B., Ho, S. K., Rama Rao, N. V. and Baird, M. H. I., 1994, "Multstage

Conutcurrent Extractor Using Vortex Rings", Accepted by Trans. Inst. Chem. Eng. (to be published in 1994).

Linden, P. F., 1973, "The Interaction of a Vortex Ring with a Sharp Density Interface: A Model for Turbulent Entrainment", J. Fluid Mechanics, Vol. 60, Pt. 3, pp. 467-480.

Lugt, H. J., 1983, "Vortex Flow in Nature and Technology", John WIley & Sons,

Maxworthy, T., 1977, "Some Experimental Studies of Vortex Rings", J. Fluid Mech., Vol. 81, pp. 465-495.

Oshima, Y., 1987, "The Game of Passing-Through of A Pair of Vortex Rings", J. phys. Soc. Japan, Vol. 45, No. 2, pp. 660-664.

Papple, M. L. C., Latto, B., Baird, M. H. I. and Shoukri, M., 1991, "Numerical Simulation of Vortex Rings Traversing a Thermally Stratified Fluid", Chem. Eng. Commun., Vol. 103, pp. 167-179.

Patankar, S. V., 1980, "Numerical Heat transfer and Fluid Flow", Hemisphere Publishing Corporation, New York.

Rama Rao, N. V., Latto, B. and Baird, M. H. I., 1994, "Liquid-Liquid Vortex Rings:

Hydrodynamics and Mass Transfer", Trans. Inst. Chem. Eng., Vol. 72, pp. 485-492.

Rogers, W. B., 1858, Amer. J. Sci., Vol. 26, pp. 246-258.

Rohatgi, A., Baird, M. H. I. and Wairegi, T., 1979, "Mixing Effects and Hydrodynamics of Vortex Rings", Canadian J. Chem. Eng., Vol. 57, No. 4, pp. 416-424.

Strange, B., 1991, "Vortex Ring Penetration through A Density Interface", Undergraduate Thesis Project, Department of Mechanical Engineering, McMaster University.

Struchayev, A. I., Kopyt, N. Rh. and Boyko, Yu. I., 1990, "Efficiency of Transport of A Dispersed Impurity by Vortex Rings" Fluid Mechanics, Soviet Research, Vol. 19, No. 2, pp. 9-18.

Turner, J. S., 1960, "Intermittent Release of Smoke from Chimneys", J. Mech. Eng. Science, Vol. 2, pp. 97-100.

Walker, J. D. A., Smith, C. R., Cerra, A. W. and Doligalski, 1987, "Impact of A Vortex Ring on A Wall", J. F. Mech., Vol. 181, pp. 99-140.

Whitehead, K. D., 1968, "The generation and Development of a Viscous Vortex Ring", Georgia Institute of Technology, School of Aerospace Engineering, Report 68-4.

Widmayer, R. S., 1972, "A Study of the Motion of Laminar and Turbulent Viscous Vortex Rings", Ph.D. dissertation, University of Maryland.